Journal of Electric Propulsion

RESEARCH Open Access

Multimode propellant discovery: a computational high-throughput screening paradigm

Shehan M. Parmar[1*], Orion Cohen[2], Kristin A. Persson[2,3], Ghanshyam L. Vaghjiani[4], Jesse G. McDaniel[1] and Richard E. Wirz[5,6*]

*Correspondence:
Shehan M. Parmar
sparmar32@gatech.edu
Richard E. Wirz
wirz@ucla.edu; richard.wirz@oregonstate.edu

Full list of author information is available at the end of the article

Abstract

The emergence of multimode propulsion (MMP) architectures for in–space propulsion shows great promise for improving the future of spacecraft mission design. However, seeking ideal propellants requires traversing a complex chemical design space that satisfies optimal chemical and electric propulsion requirements. To this end, we propose a computational, high–throughput screening framework founded upon software developed by the Materials Project and accurate, polarizable molecular dynamics (MD) force fields to discover new MMP propellants. We highlight the metric space within the scope of this framework and present a case study of a candidate ionic liquid (IL) propellant mixture composed of hydroxylammonium nitrate (HAN) and hydroxyethylhydrazinium nitrate (HEHN) to inform important paths for the future.

Keywords Multimode propulsion, Ionic liquids, High-throughput molecular dynamics, Materials discovery

Introduction

Tuning chemical structure for target engineering applications presents a complex, high–dimensional problem. Moreover, unlike smooth, convex optimization spaces, the chemical design space consists of discrete inputs (e.g., add/remove CH_2 group) that translate nonlinearly to desired outputs (e.g., thermophysical properties). Consequently, the time required to discover materials with desirable properties through trial–and–error greatly hinders technology development cycles. To this end, a number of research communities have implemented high–throughput screening (HTS) protocols to automate rapid evaluation of candidate materials. For instance, modern HTS methods for drug design can screen $10^4 - 10^5$ compounds per week to identify "hits", or compounds of biological relevance [1–4].

Despite the success of wet lab–based screening (e.g. autonomous experimentation), synthesis and replicating complex testing conditions are time and cost intensive. Thus, the advent of in silico HTS has greatly accelerated material discovery for lithium–ion

battery cathodes [5–9], hydrogen storage [10–16], carbon capture [17–22], and dielectric materials [23]. In 2011, the Materials Genome Initiative (MGI) for Global Competitiveness [24] made evident this need for deploying novel materials "at least twice as fast [and] at a fraction of the cost" through integrated computational tools [25]. One successful component of the MGI is the Materials Project [26] (http://www.materialsproject.org), an open–source, collaborative, and multi–institutional database composed of first–principles–based structural and energetic property calculations for over $150,000$ solid–state materials, i.e., the "Google of material properties" [27]. The Materials Project can be accessed by a user–friendly website or programmatically via an API and is supported by an extensive software ecosystem for organizing, executing, and analyzing high–throughput simulations of materials properties. Recent high–profile forays into materials science by large tech companies have built on the Materials Project stack. The pervasive impact of the Materials Project has led to novel machine learning methods [28], modular, user–friendly software packages [29–31] and accelerated innovation and technological development across scientific domains [32, 33].

In this paper, we leverage the successes of the Materials Project and the advancements in computational HTS methods to introduce a streamlined framework for identifying novel propellants for in–space propulsion applications. Historically, in–space propulsion has kept chemical and electric propulsion modes separate, resulting in a concomitant separation between the highest performing chemical and electric propellants. On one hand, high–thrust chemical propulsion systems require highly exothermic propellants and compatibility with heterogeneous catalysts, and hence are typically nitrogen or alcohol–rich compounds (e.g., hydrazine, N_2H_4) [34–36]. On the other hand, electric propulsion has relied on inert gases like xenon, krypton, or argon for propellants due to their low ionization energies and high atomic mass [37, 38]. Despite this contrast, recent progress in propellant chemistry and thruster architectures has enabled the emergence of multimode propulsion (MMP) concepts, in which combined chemical–electric systems share propellant and/or thruster hardware [39]. As outlined by Rovey et al. [39], the MMP paradigm extends the operating envelope of numerous space mission concepts in their "flexibility, adaptability, and responsiveness" while reducing dry mass cost through shared propulsion resources.

The primary research challenge with MMP technologies is the competing trade–offs between chemical and electric propulsion propellants, let alone the complexities involved in their individual trade–spaces irrespective of MMP. Concretely, of the number of candidate MMP propellants explored, herein we focus on a promising category of materials, ionic liquids (ILs), which have already shown spaceflight heritage in chemical and electric propulsion systems independently [40–42]. ILs are room temperature organic salts composed of cation–anion pairs that exhibit desirable properties (e.g., low vapor pressures [43], high thermal stabilities [44], high ionic conductivities [45], low toxicity [46]) for propulsion. Seeking an ideal MMP propellant, however, is obstructed by the immense chemical space of ILs: cation and anion combinations can yield up to 10^6 possible ILs. Thus, traversing the vast compositional space for the design and discovery of novel MMP propellants is ripe for advanced computational approaches.

With this motivation in mind, the objective of this work is to reduce the chemical design space of IL MMP propellants by proposing a robust, computational framework to accurately quantify key thermophysical parameters via first–principles calculations.

To this end, the paper is outlined in three main sections. In Section "Related work", we discuss the valuable insights learned from past chemical, electric, and multimode propulsion studies to develop design principles and guide property calculations of interest. Then, in Section "Approach: computational high–throughput screening", we outline the novel, computational HTS framework composed of the software stack drawn from the Materials Project and molecular dynamics (MD) simulation methods. Finally, in Section "A case study: binary [HAN][HEHN] mixtures" we share results of a case study for a set of binary protic ionic liquid (PIL) mixtures to highlight the insights and future opportunities with such a computational paradigm. We emphasize the motivation of this work exists at the intersection of MMP technology development and fundamental IL science exploration. Computational high–throughput screening of ILs will impact fields beyond electric and in–space propulsion, as ILs are readily used as battery electrolytes [47–50], in water desalination [51], and even in carbon capture [52].

Related work

Key multimode performance parameters

We begin this section by reviewing the multimode rocket equation introduced in previous studies by Berg [53, 54], Donius [55, 56], and Rovey et al. [39]. Given the separate nature of chemical and electric propulsion (CP and EP, respectively) modes, the "EP fraction", f_{EP}, is commonly defined as shown in Eq. 1:

$$f_{EP} = \frac{\Delta V_{elec}}{\Delta V}\ , \tag{1}$$

where the EP mode contribution towards the total delta–V, ΔV, is quantified. Consequently, the multimode rocket equation [39, 53–56] is defined by Eq. 2,

$$\frac{m_f}{m_o} = e^{-(\Delta V / I_{sp,mm} g_o)} \tag{2}$$

where the initial and final mass is m_o and m_f, respectively, and the effective multimode specific impulse is

$$I_{sp,mm} = \left[\frac{1 - f_{EP}}{I_{sp,chem}} + \frac{f_{EP}}{\eta_v I_{sp,elec}}\right]^{-1}, \tag{3}$$

where the chemical and electric specific impulse are given by $I_{sp,chem}$ and $I_{sp,elec}$, respectively, and "mission planning efficiency" is η_v, for which typical Earth–orbiting missions, these values range from 0.45 to 0.65 [39, 57, 58]. The coupling of optimal electric propulsion specific impulse with chemical mode specific impulse has been previously discussed [54, 57]; nonetheless, Eq. 3 highlights holistically how multimode performance is inherently linked to propellant properties. Concretely, by linking (to reduced order) specific impulse and effective exhaust velocity ($u_e = I_{sp} g_o$), CP performance can be evaluated by neglecting pressure thrust and assuming isentropic expansion, resulting in Eq. 4,

$$I_{sp,chem} = \frac{1}{g_o}\sqrt{2\frac{\bar{R}}{\bar{M}}\frac{\kappa}{\kappa - 1}T_0\left[1 - \left(\frac{p_e}{p_o}\right)^{\frac{\kappa}{\kappa-1}}\right]}, \tag{4}$$

where $\bar{R}$ is the universal gas constant, κ is the specific heat ratio, $\bar{M}$ is the ejected propellant species molecular weight, T_0 is the combustion chamber temperature, and p_o and p_e are combustion chamber and exit pressures, respectively. In contrast, most state–of–the–art EP systems use electrostatic acceleration of charged particles based on the electric potential energy of the power source, and ignoring non–idealities results in Eq. 5

$$I_{sp,elec} = \frac{1}{g_o}\sqrt{2V_B\frac{q}{m_i}}, \tag{5}$$

where V_B is the beam voltage, and q/m_i is the charge–to–mass ratio of the accelerated particle *i*. In the case of electrospray thrusters, an exemplary IL–based EP system commonly considered attractive for monopropellant MMP, the charge–to–mass ratio is ubiquitously linked to the emitted current, I_{em}, which has been shown to be theoretically and experimentally linked to physical liquid properties by the proportionality in Eq. 6: [59–63]

$$\frac{q}{m_i} \propto \frac{I_{em}}{\rho Q} \propto \frac{1}{\rho}\sqrt{\frac{\gamma\sigma}{\varepsilon Q}}, \tag{6}$$

where propellant density, ρ, surface tension, γ, electrical conductivity, σ, dielectric constant, ε, and flow rate, Q, contribute to the overall EP performance. The implications of Eqs. 4–6 are clear: the liquid properties that contribute to MMP performance differ fundamentally between modes, where $I_{sp,chem}$ depends predominantly on chemical potential energy while $I_{sp,elec}$ depends on a combination of bulk phase static, electrical, and transport properties.

Molecular structure—the origin of propellant properties

Section "Key multimode performance parameters" underpins the connection between IL propellant molecular structure and MMP performance. Throughout this work, *molecular structure* refers to the atomic connectivity and intramolecular geometry of individual molecular ions, while chemical composition denotes the relative abundance of these species within the multimode propellant formulation. In later sections, we will focus on *bulk* or *liquid* structure, a macroscopic manifestation of molecular structure. For chemical propulsion, high adiabatic flame temperatures and low average molecular weights of combustion species are desirable, as these increase exhaust velocity and specific impulse [64]. Both quantities are ultimately rooted in chemical structure, where molecular weight is a direct consequence of molecular structure whereas adiabatic flame temperature more subtly depends on bond thermochemistry. In general, the adiabatic combustion temperature is found by applying conservation of mass and energy to the reacting system. The standard heat of reaction is

$$\Delta_r H^0 = \sum_j \left[n_j(\Delta_f H^0)_j\right]_{\text{products}} - \sum_j \left[n_j(\Delta_f H^0)_j\right]_{\text{reactants}}, \tag{7}$$

where n_j is the molar concentration of each species *j*. The combustion temperature, T_0, is then determined by the combustion enthalpy, and $\Delta_f H^0$ is the enthalpy of formation.

$$\Delta_r H = \sum_{j=1}^{m} n_j \int_{T_{\text{ref}}}^{T_0} C_{pj} dT = \sum_{j=1}^{m} n_j \Delta h_j |_{T_{\text{ref}}}^{T_0}, \tag{8}$$

where Δh_j is the enthalpy increase per species from the initial reference temperature, T_{ref}, and C_{pj} is the species molar specific heat at constant pressure [65]. While a complete review of methods for determining T_0 is outside the scope of this work, a number of computational and iterative procedures have long been implemented, supporting the hypothesis that combustion mechanisms arise, in part, from molecular structure and composition [59, 66–72]. For electric propulsion, Eqs. 5 and 6 connect MMP performance to bulk phase and interfacial properties: density, conductivity, and surface tension. Significant research has been dedicated to establishing so–called structure–property relationships that elucidate how chemical structure (e.g., through cation alkyl chain length, degree of anion charge delocalization, etc.) tune these electrospray performance–driving properties [73–82]. From the results of Eq. 6, one can define an electrospray criterion, $\sqrt{\gamma\sigma}/\rho$ for an assumed product $Q * \varepsilon$. Fig. 1 illustrates the dependence (to reduced order) of this criterion to molecular structure and composition. This heatmap reveals that ILs that maintain moderately large surface tension and conductivities with relatively low densities "score" the highest on this metric (under otherwise identical electrospray emitter and electric field conditions).

Moreover, Fig. 2 adds chemical structure trends for viscosity, which notably constrains electrospray flow rate via its influence on hydraulic resistance [99–101]. While conductivity and bulk viscosity are generally expected to follow an inverse trend, differences in molecular structure and composition reveal quantitative subtleties as well as inform how structure modulates global trends.

Figure 3 illustrates that IL propellants cannot be optimized with respect to a single property or metric alone. By juxtaposing conductivity, surface tension, and

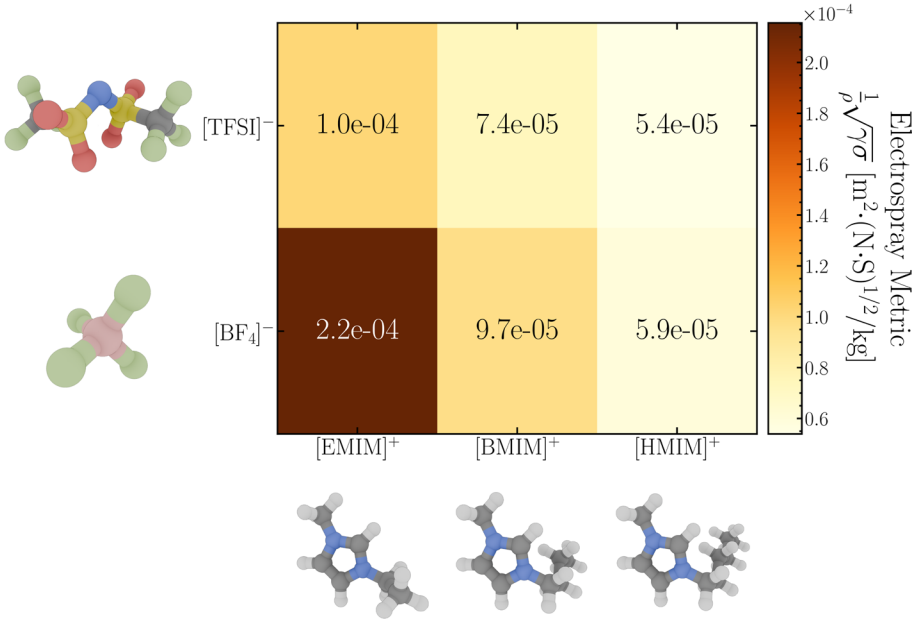

Fig. 1 Electrospray propellant performance metric, $\sqrt{\gamma\sigma}/\rho$, based on density, ρ, surface tension, γ, and conductivity, σ, for six, neat imidazolium-based ionic liquids. Properties are obtained from experimental values across the literature [83–97]

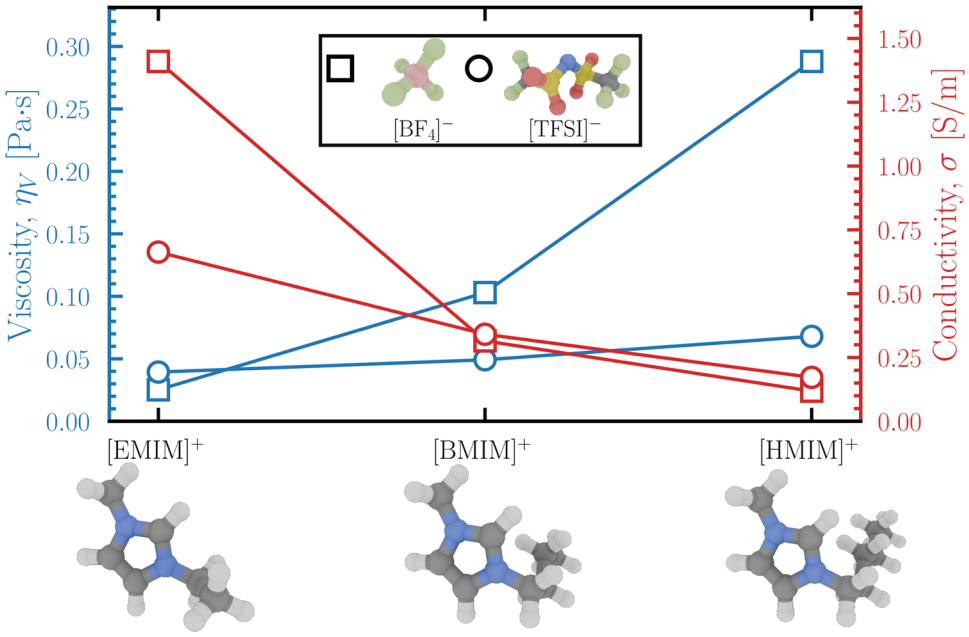

Fig. 2 Bulk viscosity, η_V, and conductivity, σ, of imidazolium–based ILs as a function of cation alkyl chain length and anion structure. All values obtained from experiments at ~ 300 K [83–92, 98]

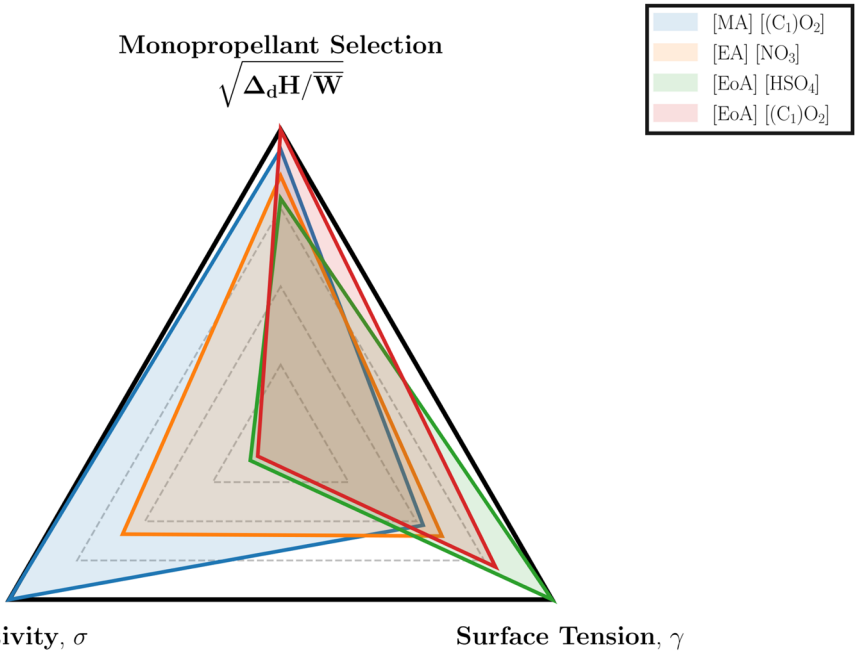

Fig. 3 Radar plot of three multimode monopropellant screening criteria, conductivity, surface tension, and "monopropellant selection metric", of four protic ILs defined and measured by Fonda–Marsland and Ryan [102]

Fonda–Marsland and Ryan's monopropellant selection metric [102], the radar plot highlights that performance in one mode often comes at the expense of another. ILs that excel as monopropellants may perform poorly in electrosprays, and vice versa, underscoring the multi–objective nature of MMP propellant selection. Thus, given the vast chemical space of ILs and their binary mixtures, simple structural and compositional heuristics are quickly outpaced by the diversity of possible trade–offs. To this end, the

high–throughput molecular simulation tools presented in this work provide a practical path to systematically computing important propellant properties, including density, conductivity, viscosity, and interfacial properties; thereby achieving the objectives of propellant exploration and selection by increasing the search space and guiding targeted experimental campaigns toward promising propellant candidates.

Candidate Ionic liquid MMP propellants

Unsurprisingly, insights from Section "Key multimode performance parameters" have led to a natural demarcation in the nature of IL propellants for either chemical or electric propulsion applications. For instance, ILs used successfully in CP systems are often categorically energetic ILs (EILs) due to their high heats of combustion, relatively high thermal stability, low toxicity, and low vapor pressures [103]. Accordingly, many examples of EIL compounds are characteristically nitrogen rich, where azide, dinitramide, dicyanamide, and nitrocyanamide and ammonium, aminotriazole, and aminotetrazole are all examples of anions and cations, respectively [104–114]. CP propellant blends, or mixtures, include other constituents that ultimately tune performance–driving properties. These include, for instance, ammonium dinitramide (ADN)–based monopropellants like FLP–106 [115] and LMP–103S [116] and hydroxylammonium nitrate (HAN)–based formulas like AF–M315E [117] and SHP163 [40]. In parallel, the development of electric propulsion systems, like electrospray thrusters, depend on highly mobile and structurally compact cation/anion pairs. Hence, significant research has been done for [EMIM][BF_4] [118], [EMIM][TFSI] [119], [BMIM][DCA] [120], and other similar ILs. While chemical and electric propellants fundamentally differ, a number of studies have begun characterizing combinations of the two. For example, such mixtures include [EMIM][$EtSO_4$][HAN] [121–123] and [EMIM][$EtSO_4$][AN] [122], in which the linear burn rate, synthesis procedures, and catalytic compatibility were assessed. The first conceptual screening of hundreds of candidate neat ILs was conducted by Fonda–Marsland and Ryan via an experimental approach [102]. In this study, 170 room–temperature ILs (RTILs) were screened based on unique criteria for electric, $\sqrt{\gamma\sigma}$, and chemical propulsion, $\sqrt{\Delta_d H/\bar{W}}$, where $\Delta_d H$ is the enthalpy of decomposition and $\bar{W}$ is the propellant mass. These findings identified 15 aprotic and protic ILs that showcased promise and feasibility based on their fundamental properties. These ILs include common cations, such as [C_1Mim], [EMIM], [BMIM], [MA], [EA], and [PA], and anions, such as [TFSI], [BF_4], [NO_3], and [DCA].

While other HAN–based mixtures have also been explored [124, 125], the general availability of fundamental studies of relevant systems is relatively limited. Nonetheless, across the literature, it is clear that mixture chemistry presents added bulk phase complexity that is not easily rationalized by individual components [126]. Furthermore, solubility and phase behavior is often a rather subtle balance of hydrophilic and hydrophobic domains present in the IL, resulting in the reportedly non–intuitive mixing behavior among many "double salt ILs" (DSILs) [127]. Thus, these previous insights further substantiate the importance of high–throughput simulation methods to support experimental campaigns to better understand MMP propellants' design principles.

Approach: computational high–throughput screening

First–principles–based computational methods

Molecular Dynamics and force field selection

The overall high–throughput screening framework relies on the use of accurate, first–principles–based molecular dynamics (MD) simulations. Unlike the current Materials Project database, where solid–state properties are computed using density functional theory (DFT) calculations, the desired bulk phase, liquid properties in this work demand extensive statistical sampling and hundreds to thousands of molecules in each simulation to properly obtain short– and long–range behavior. To this end, we use modern MD practices within the overarching framework.

The crux of any MD simulation is in the force field, or the functional form that characterizes the interatomic potential. Classical MD force fields account for bonded (i.e., bonds, angles, dihedrals) and nonbonded (i.e., 12–6 Lennard–Jones and Coulomb potentials) terms via a series of empirical or first–principles–based parameters. We highlight that for ILs, force field selection is a significant challenge given the complex behavior of charged molecules in a condensed–phase system. For the purposes of this computational framework, we approach force field selection with two prominent categories in mind: polarizable and nonpolarizable force fields.

We emphasize that the workflow proposed offers modularity and interchangeability between available force fields. Previous nonpolarizable force fields used for ILs include OPLS–AA [128], AMBER [129], and recently, force fields parameterized using machine learning methods, such as espaloma [130]. While a number of thermophysical properties have been accurately reproduced via nonpolarizable force fields, we emphasize the need for polarizable force fields like APPLE&P [131], CL&Pol [132, 133], or SAPT–FF [83], in which the molecular response to local electric fields is explicitly modeled through induced atomic dipoles. Based on significant literature [134], nonpolarizable force fields systematically miss a number of key static and transport properties crucial for the proposed metric space in this work. The inconsistent macroscopic properties predicted by nonpolarizable force fields is rigorously explained by the requirement that ILs, being electrolytes, satisfy electroneutrality and screening conditions [135]. Electroneutrality requires the following constraint on the ion–ion, radial distribution functions

$$\sum_{\mu} \int_0^{\infty} 4\pi r^2 \rho_{\mu} q_{\mu} g_{\nu\mu}(r) d\mathbf{r} = -q_{\nu} \tag{9}$$

where μ and ν are cations or anions, and $g_{\nu\mu}(r)$ is the ion–ion radial distribution function (RDF). In essence, Eq. 9 illustrates that a tagged ion must be surrounded by an equal and opposite "charge cloud" to ensure electroneutrality.

Also, being an electrolyte, the IL is expected to exhibit perfect electrostatic screening, at least in the asymptotic limit. This condition is quantified by the asymptotic requirement of the dielectric response, which in Fourier–space is $\lim_{k\to 0} \epsilon(k)^{-1} = 0$. This behavior is analogous to perfect conductors (e.g. metals) that screen electric fields instantaneously, usually quantified by $\epsilon^{-1} = 0$ without a lengthscale specification. Utilizing statistical mechanical linear response theory, this screening requirement is translated to conditions imposed on the pairwise correlation functions of the IL, or their Fourier space analogues, structure factors. These screening requirements are known as

the second–moment Stillinger–Lovett sum rule or "perfect screening condition" [136–140], which takes the general form

$$\frac{4\pi}{k_B T} \lim_{|\mathbf{k}|\to 0} \frac{S_{zz}(\mathbf{k})}{\mathbf{k}^2} = 1 - \frac{\epsilon_\infty - 1}{\epsilon_\infty}, \tag{10}$$

where ϵ_∞ is the infinite frequency dielectric response. S_{zz} is the charge–correlation structure factor,

$$S_{zz}(\mathbf{k}) = \frac{1}{V}\langle \hat{\rho}_Z(\mathbf{k})\hat{\rho}_Z(-\mathbf{k})\rangle, \tag{11}$$

where $\langle \cdots \rangle$ denotes an ensemble average, $\mathbf{k}$ is the wavevector, and

$$\hat{\rho}_Z(\mathbf{k}) = \sum_{i=1}^{N} q_i e^{i\mathbf{k}\cdot\mathbf{r}_i} \tag{12}$$

is the Fourier component of the microscopic charge density, where q_i is the partial atomic charge, $\mathbf{r}_i$ is the position of the atom i, and N is the total number of atoms in the system.

It is expected that ILs and electrolytes at equilibrium should obey Eq. 10, at least away from a phase transition or critical point. The interpretation of S_{zz} is instrumental to understanding ILs: the Coulomb interaction length–scales that govern bulk phase arrangement of ions are directly quantified by the charge correlation structure factor. The key difference in simulations of polarizable and nonpolarizable force fields is the right hand side of Eq. 10, since polarizable force fields have $\epsilon_\infty \neq 1$ while nonpolarizable force fields have $\epsilon_\infty = 1$. McDaniel and Yethiraj have shown that the differences in this fundamental limit on the structure factors propagates to substantial deviations in ion structuring, on both sub–nanometer and nanometer lengthscales as predicted by polarizable versus nonpolarizable force fields [141]. Thus for simulations of ILs, correct prediction of S_{zz} and its asymptotic limit are instrumental to the force field's predictive capability of macroscopic and transport properties [134, 141]. We will later comment on the importance of S_{zz} in understanding relevant solvation and miscibility behavior in ILs.

Software pipeline and infrastructure

Materials Project software stack and base libraries

Running high–throughput simulations requires setting up diverse sets of simulations, managing their execution on high performance computers (HPC), and analyzing and organizing the simulation output. The Materials Project stack provides a sophisticated framework for managing these high–throughput campaigns, which can quickly become messy and burdensome when run on the scale of tens or hundreds of thousands of simulations. For example, running a molecular dynamics simulation requires assembling a set of force field parameters, synthesizing them into a single input file, using Packmol [142] to generate an initial configuration, executing the job on an HPC, and running analysis scripts. Traditionally, each step would be performed manually, at best linked together by bespoke analysis scripts, essentially precluding high–throughput approaches. For this reason, MD has acquired a reputation for being difficult, time–consuming, and tedious.

Instead, implemented in the Materials Project stack, ~80 lines of Python code can execute the end–to–end MD workflow.

Basic input and output operation

Pymatgen [29] and Atomate2 [31, 143], building on the Open Force Field stack [144], implement utilities for configuring molecular dynamics systems from simple user inputs. The minimal input is a Python dictionary specifying the structure and count for each molecule. Molecular structures in this work are specified using SMILES (Simplified Molecular Input Line Entry System), which provide a compact, text–based description for arbitrary molecules [145]. While SMILES is widely used across the cheminformatics space, it does not offer three–dimensional coordinate information, stereochemistry, and conformational details. To generate simulation–ready, 3D structures, we leverage the Open Force Field toolkit which handles geometry reconstruction and optimization from SMILES [146, 147]. Users can select the force field, partial charges, initial geometries, and metadata as needed. Atomate2 evolves the system in OpenMM [148] with pre–set and custom workflows while tracking the trajectory and state. Here, the user can configure various simulation parameters such as temperature, pressure, time step, etc. While running, the positions of all atoms in the system are recorded in a trajectory file (by default, a '.dcd') along with other state variables such as the system energy, volume, and pressure. Emmet automatically calculates a wide variety of properties from the system output using MDAnalysis [149] and SolvationAnalysis [150]. Users can easily upload these to a MongoDB database for easy querying, access, and sharing. The full workflow is detailed in Fig. 4. Each package is designed to be extensible for new simulations, new workflows, and new analyses.

Defining metrics

In this section, we highlight the utility of MD as a method to accumulate important properties of IL short– and long–range structure, electrostatics, and dynamics. It is

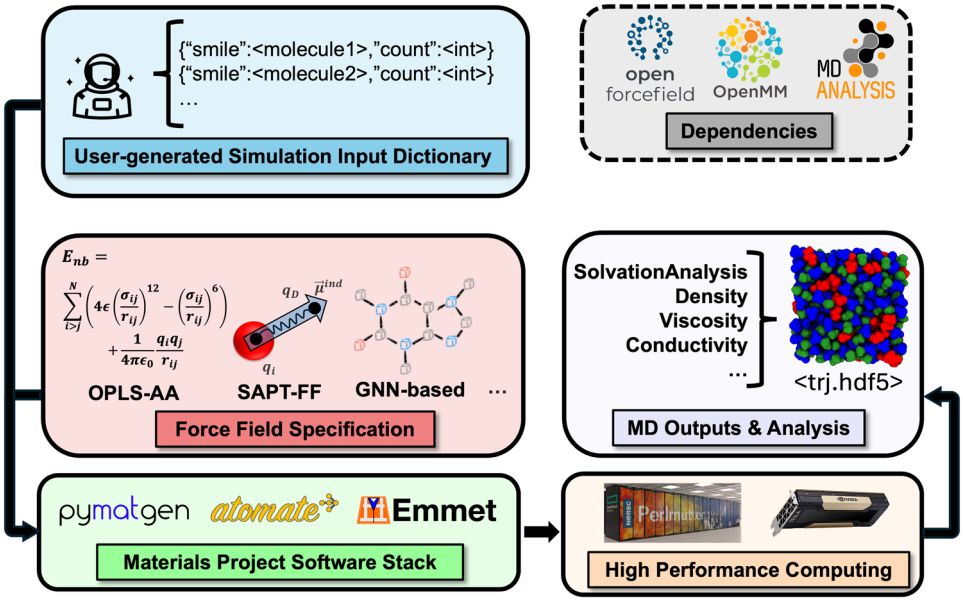

Fig. 4 Overarching computational high–throughput screening framework

important to note that classical MD simulations report equilibrium properties and cannot directly quantify energetic properties like ignition time delays or enthalpies of combustion. However, as will be shown in Section "A case study: binary [HAN][HEHN] mixtures" (*vide infra*), hydrogen bonding behavior can be characterized by the following structural analyses, a primary indicator of proton transfer reactions relevant in protic ILs (PILs) [151–153].

To this end, we aim to acquire a database of simulated properties for a range of IL mixtures with varying concentrations and temperature conditions. It should be noted that each equilibrium MD simulation is carried out within a specific statistical ensemble (e.g., constant *NVT*, *NVE*, or *NPT*) at a defined thermodynamic state point [154, 155]. Convergence of structural and transport properties requires monitoring the stability of key system observables such as density and potential energy. We refer the reader to comprehensive reviews and textbooks for detailed discussions of ensemble workflows and equilibration strategies leveraged in this work [83, 84, 156–162]. Generally, MD simulations calculate time–averaged properties to characterize local and long–range structure. These include radial distribution functions (RDFs), $g(r)$, which provide the average number density of particles around a reference particle as a function of radial position. The coordination number, $N(r)$, is proportional to the integral of the $g(r)$ by Eq. 13

$$N(r) = \int_0^r 4\pi\tilde{r}^2\hat{\rho}g(\tilde{r})d\tilde{r}, \tag{13}$$

where $\hat{\rho} = N/V$ is the average number density of the observed atom (in $Å^{-3}$). The $g(r)$ provides detailed information of pairwise correlations that compliment experimental X–ray or neutron scattering structure factors, which can also be computed via MD simulations [141]. Similar distribution functions that quantify conformation diversity or angular arrangement near coordination sites can be acquired by dihedral and angular distribution functions, (ADFs and DDFs), respectively.

Along with structural properties, thermophysical, electrostatic, and transport properties are also of significant interest for MMP performance evaluation. Unlike molecular solvents, ILs have large liquid cohesive energies due to strong Coulombic interactions between cation/anion pairs, giving rise to their unique thermophysical and transport properties. The liquid cohesive energy, E_{coh} can be computed by Eq. 14

$$E_{cohesive}(T) = \frac{1}{N_{ionpair}} E_{liquid}(T) - E_{cation}(T) - E_{anion}(T). \tag{14}$$

While E_{coh} cannot be determined experimentally due to the challenge of gas phase ion binding, the enthalpy of vaporization can be computed by Eq. 15,

$$\Delta H_{vap}(T) = \frac{1}{N_{ionpair}} \left[E_{vapor}(T) - E_{liquid}(T)\right] + RT. \tag{15}$$

The charge correlation structure factor S_{zz} provides rigorous characterization of the electrical properties of the IL. Analysis of $S_{zz}(k)$ (and its dynamic analogue, $S_{zz}(k,t)$ [135]) provides information on electrostatic screening, [141] solvation behavior [163], and miscibility [164]. For instance, McDaniel and Verma [164] show that the S_{zz} of *pure* ILs can unambiguously classify them into hydrophobic and hydrophilic categories based on signatures in the $\sim Å^{-1}$ wavevector region.

Furthermore, transport properties are also made accessible by MD simulations. The Einstein relation for the self–diffusion coefficient is given by Eq. 16

$$D_s = \frac{1}{6} \lim_{t\to\infty} \frac{d}{dt} \langle |\bar{r}(t) - \bar{r}(0)|^2 \rangle, \tag{16}$$

where the bracketed quantity is the mean squared displacement (MSD). The diffusion–viscosity relationship is often related by the Stokes–Einstein equation that yields the proportionality, $D_s \propto T/\eta_V$, where η_V is the bulk viscosity. The shear viscosity can be computed via MD simulations directly, however, and is given as a function of the elements of the pressure tensor, $P_{\alpha\beta}$, [154]

$$\eta = \frac{V}{k_B T} \int_0^\infty dt \langle P_{\alpha\beta}(t) P_{\alpha\beta}(0) \rangle, \tag{17}$$

where k_B is the Boltzmann constant, T is the temperature, and V is the system volume. Similarly, the total ionic conductivity is defined by Eq. 18 [140],

$$\sigma = \lim_{t\to\infty} \frac{1}{6tVk_BT} \sum_{i,j}^{n} \langle (q_i[r_i(t) - r_i(0)]) \cdot (q_j[r_j(t) - r_j(0)]) \rangle, \tag{18}$$

where charges q and positions r are used to sum over all combinations of "i, j" of cations and anions in the systems. Moreover, the total ion conductivity in Eq. 18 can be decomposed to capture correlations in the motion of the respective species.

In summary, the MMP propellant property predictions within the scope of this work are provided below:

Characterization of local structure

- radial distribution functions (RDFs), $g(r)$
- running coordination numbers, $N(r)$
- angular distribution functions (ADFs)
- dihedral distribution functions (DDFs)
- X–ray and neutron scattering structure factors

As we highlighted in Parmar et al. [165], the density specific impulse remains a key characteristic for both multimode propulsion thruster performance and underlying mission flexibility [39]. Thus, density remains both the most convenient and pertinent initial screening parameter at the top of the conceptual HTMD "funnel", as shown in Fig. 5.

Static and transport properties

- density, ρ
- liquid cohesive energy, E_{coh}
- enthalpy of vaporization, ΔH_{vap}
- charge correlation structure factor, S_{zz}
- self–diffusion coefficients, D_s, D_+, D_-
- bulk, η_V, and shear viscosity, η
- conductivity, σ

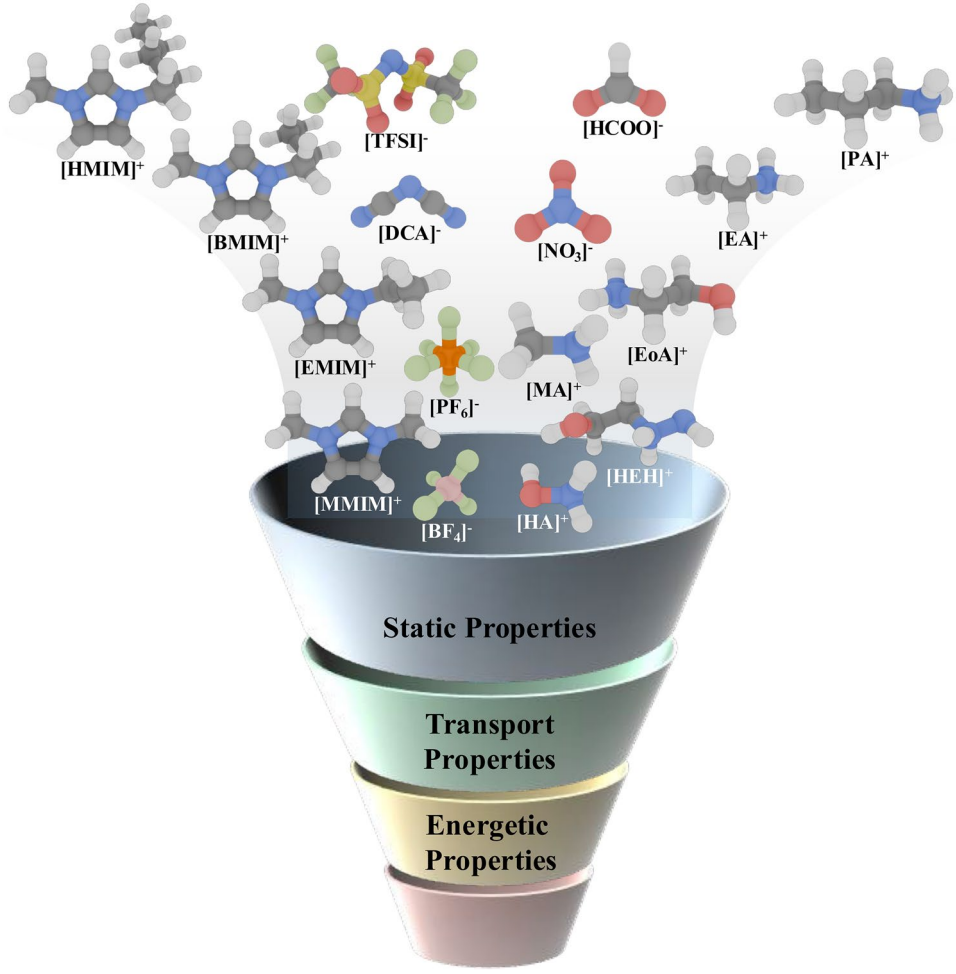

Fig. 5 Screening workflow with hierarchical approach to computing thermophysical properties via molecular dynamics

A case study: binary [HAN][HEHN] mixtures

Herein, we present a case study based on our work in Parmar et al. [165] to showcase a series of exemplary results representative of that sought after in our overarching, high–throughput framework. In particular, we investigate mixtures of two, task–specific ILs, HAN ($NH_3OH^+ \cdot NO_3^-$) and HEHN ($HOCH_2CH_2N_2H_4^+ \cdot NO_3^-$); in a propellant blend, HAN and HEHN complement each other as an ionic oxidizer and fuel, respectively. As shown in Fig. 6, four [HAN][HEHN] systems at 25, 50, and 75% HAN by weight and neat HEHN for comparison were simulated using the polarizable MD force field, APPLE&P [131]. Simulations were performed in the *NPT* ensemble at room temperature (300 K) and standard pressure (1 atm). The number of molecules and box sizes were determined by mole fraction; for example, at $\chi = 0.0$, the neat HEHN system contained $400\ HEH^+$ and $400\ NO_3^-$. Packmol [142] was used to construct an initial box approximately 1.5 times larger than the equilibrated volume. Equilibrated simulation cells had a length of $\sim 30 - 40$ Å. For further discussion of computational methods and verification, we refer the reader to Parmar et al. [165].

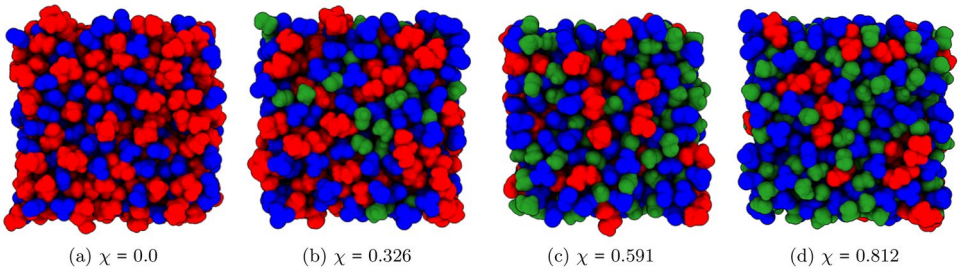

(a) χ = 0.0 (b) χ = 0.326 (c) χ = 0.591 (d) χ = 0.812

Fig. 6 Equilibrium snapshots of bulk phase [HAN][HEHN] liquid mixtures with varying mole fractions, χ, of [HAN]. Red, blue, and green colored molecules correspond to hydroxyethylhydrazinium cation (HEH^+), nitrate anion (NO_3^-), and hydroxylammonium cation (HA^+), respectively

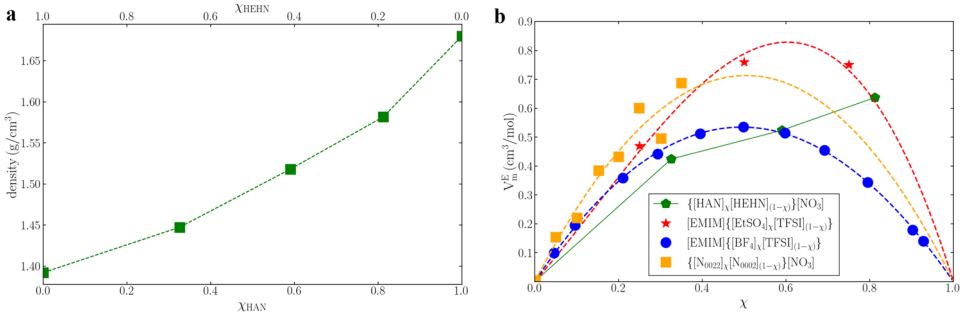

(a) $\rho(\chi)$ (b) $V_M^E(\chi)$

Fig. 7 (**a**) Simulation results for density as a function of HEHN and HAN mole fraction at room temperature (the 50–50% [HAN][HEHN] was conducted at 293 K to match the experimental measurement while every other "room temperature" calculation was at 298 K). Density of pure HAN ($\chi_{\mathrm{HEHN}} = 0.0$) is based on an experimental reference value of 1.68 g cm^{-3} for anhydrous HAN [166], for which no temperature value was reported but is expected to be near the HAN melting point, $44 - 48^{\circ}\mathrm{C}$ [167]. b) Calculated excess molar volume of [HAN][HEHN] mixture. Experimental comparison includes three–ion DSIL mixtures of 1–ethyl–3–methyl–imidazolium (EMIM) cations with ethylsulfate ($\mathrm{EtSO_4}$) and bis(trifluoromethylsulfonyl)imide (TFSI), EMIM with tetrafluoroborate ($\mathrm{BF_4}$) and TFSI, and nitrate anions ($\mathrm{NO_3}$) with ethylammonium ($\mathrm{N_{0002}}$) and diethylammonium ($\mathrm{N_{0022}}$) cations. Associated Redlich–Kister curve fits as a function of mole fraction are provided for systems with sufficient data points (dashed lines)

[HAN][HEHN] density and mixture compatibility

Among the properties studied, density and excess molar volumes as a function of mole fraction are discussed first, as shown in Fig. 7. As shown in Eq. 19, V_m^E is effectively the difference in the actual mixture molar volume and the individual constituent molar volumes,

$$V_m^E = \frac{\chi_{\mathrm{HAN}} M_{\mathrm{HAN}} + \chi_{\mathrm{HEHN}} M_{\mathrm{HEHN}}}{\rho_{[\mathrm{HAN}][\mathrm{HEHN}]}} - \frac{\chi_{\mathrm{HAN}} M_{\mathrm{HAN}}}{\rho_{\mathrm{HAN}}} - \frac{\chi_{\mathrm{HEHN}} M_{\mathrm{HEHN}}}{\rho_{\mathrm{HEHN}}}, \tag{19}$$

where χ, M, and ρ are the mole fractions, molar masses, and densities of the constituents in the subscripts, respectively [127]. As expected, the density as a function of mole fraction, $\rho(\chi)$, displays an inverse relationship with increasing χ_{HEHN}; or rather, at larger values of χ_{HAN}, the system experiences stronger cation–anion Coulombic attraction given the compact, polar nature of the HA^+ cation. As a result, introducing HAN into the mixture can effectively increase the density by up to ~20%. We highlight that, while density predictions from classical MD are typically ancillary, in the context of MMP propellant assessment, they have significant implications from a performance standpoint.

For instance, as addressed by Freudenmann and Ciezki [168], AF–M315E—a propellant blend predominantly composed of HAN, HEHN, and water—outperforms hydrazine in its density specific impulse by ~50%. Through Fig. 7a, this is directly rationalized by MD simulations: the compact HA^+ and the bulky HEH^+ cations complement each other structurally, ultimately enabling a relatively stable, condensed–phase mixture at varied concentrations. Nonetheless, Figure 7a highlights how $\rho(\chi)$ is nonlinear and that to tune a single performance parameter like ρI_{sp} requires a subtle balance of molecular components.

Moreover, an a priori estimation of [HAN][HEHN] miscibility would suggest that, given both species are polar, mixtures therein should be compatible; Fig. 7b suggests otherwise. The relatively large and positive excess molar volumes indicate that certain concentration regimes may undergo non–ideal mixing behavior, such as phase separation. Similar studies of excess molar volumes of ILs attribute non–idealities to the substantial difference in molecular weight and volume of the uncommon ion (i.e., 34.04 g mol^{-1} for HA^+ vs. 77.11 g mol^{-1} for HEH^+) [169, 170]. Evidently, the relationship between concentration and phase behavior is complex. Thus, we highlight the importance of both high–throughput software infrastructure and available experimental data to support exploration of a wider range of mixtures beyond simple, binary systems.

Fundamental electrostatic and transport behavior

It is well known that ions in ILs and electrolytes more generally arrange based on either hard–packing or electrostatic screening [135]. The charge–neutrality sum rule introduced in Eq. 10 indicates that in the limit as $r \to \infty$, the sum of the charge for a given species should approach unity, i.e., $|-q^{\nu}_{sum}| = 1$. Fig. 8a shows this behavior, where the cation and anion species result in charge oscillations up to 15 Å for both the neat HEHN and the 50–50% [HAN][HEHN] systems. These charge oscillations are macroscopically indicative of concentric spheres of alternating charge that determine the long–range liquid behavior. In the case of neat HEHN, the HEH^+ introduces charge delocalization that manifests in its increased length–scale of $q^{HEH^+}_{sum}$ (red curves) relative to $q^{HA^+}_{sum}$ (green curves).

The power of analyzing ILs through Fig. 8a is highlighted by its connection to transport properties, like the self–diffusion coefficient introduced in Eq. 16, D_s, and shown in

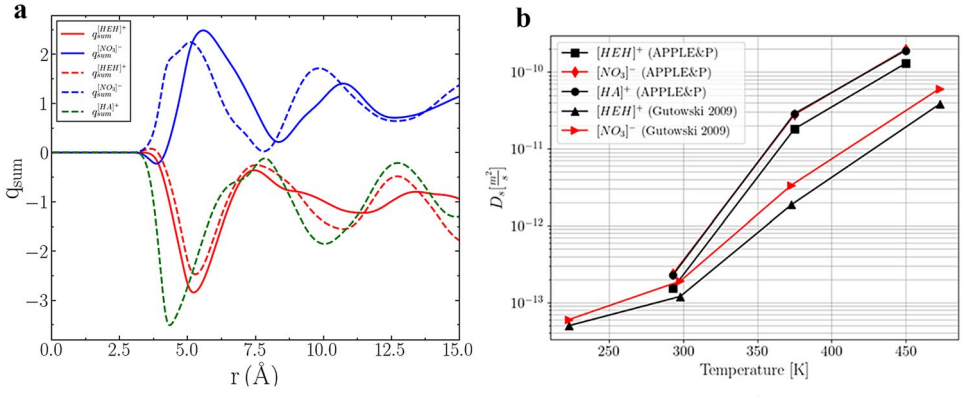

(a) $q^{\nu}_{sum}(r)$ (b) $D^{i}_{s}(T)$

Fig. 8 (**a**) Charge oscillations (Eq. 9) in a neat HEHN (solid lines) and 50–50% [HAN][HEHN] (dashed lines) system. (**b**) Self–diffusion coefficients calculated for each species in comparison to Gutowski et al. [171]

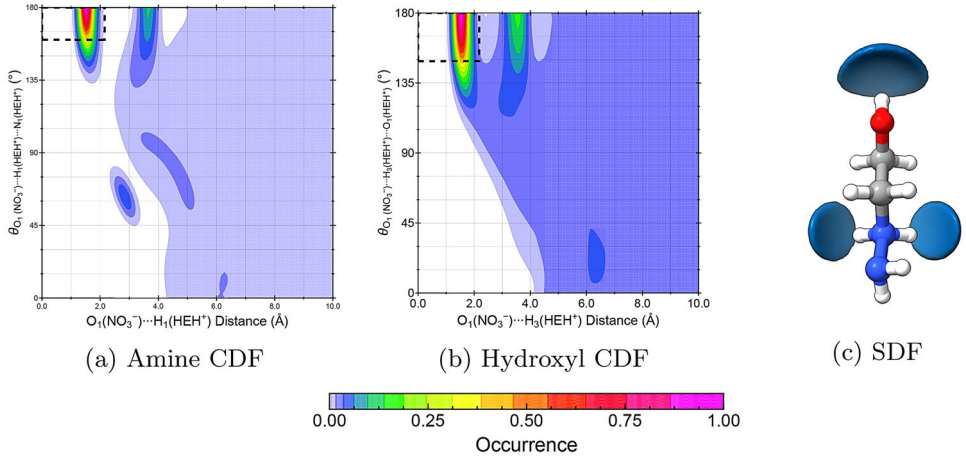

Fig. 9 (**a** and **b**) Combined distribution functions (CDFs) of $O\cdots H$ RDFs and $O\cdots H\cdots N$ (**a**) or $O\cdots H\cdots O$ (**b**) ADFs for bulk phase 50–50% [HAN][HEHN] mixture. (**c**) Spatial distribution functions (SDFs) in [HAN][HEHN] mixtures around the HEH^+ cation. Ocean blue isosurfaces indicate preferential positioning of the nitrate oxygen with respect to the cation reference frame. Reprinted (adapted) with permission from J. Phys. Chem. B 2023, 127, 40, 8616–8633. Copyright 2026 American Chemical Society

Fig. 8b. As Roy et al. [172] describe, the anti–correlated charge oscillations along with the strong cohesive energies of ILs result in a "disordered lattice" behavior of the bulk phase; macroscopically, this results in relatively small self–diffusion coefficients on the order of $10^{-13} - 10^{-10}$ m^2 s^{-1}; compared to literature values of common ILs, this is relatively small [173, 174]. While limited experimental data is available for [HAN][HEHN] mixtures, the small self–diffusion coefficients are supported by the remarkably high viscosities of similar liquids, i.e., 147 cP for 2–HEH (2–hydroxyethylhydrazine) [175]. As will be further discussed in Section "Behavior of hydrogen bonding", the slow dynamics and low ion mobility present in bulk phase [HAN][HEHN] is connected to the Coulombic interactions characterized by strong hydrogen bonds.

Behavior of hydrogen bonding

Finally, we present the importance of hydrogen bonding elucidated by simulation results. While extensive discussion is provided in Parmar et al. [165], here we summarize the implications of numerous distribution functions (i.e., radial, angular, spatial) on the protic nature of HEHN and [HAN][HEHN] systems. Figs. 9a and 9b show combined distribution functions (CDFs) in which the x– and y–axes are radial and angular distribution functions (ADFs and RDFs), respectively. The RDFs show average coordination distances below 2.0 Å of the HEH^+ amine (9a) and hydroxyl (9b) hydrogen with the nitrate oxygen; the ADFs show the hydrogen bond angle between ~150 and 180° of the $O\cdots H\cdots N$ (9a) or $O\cdots H\cdots O$ (9b) coordination sites. The CDFs largely convey the geometric conditions of hydrogen bonding, or a "point along the proton transfer coordinate." [176] The dense, red region in the top left corner of the CDFs suggest that relative to previously reported hydrogen bonds, the strength and linear directionality can be classified as "moderately" strong "ionic" bonds [176, 177]. The spatial distribution function (SDF) in Fig. 9c shows ocean blue isosurfaces of dense regions where the nitrate anion's oxygen atoms coordinate: the amine and hydroxyl coordination sites.

Figure 9 provides holistic information regarding the inherent, thermal decomposition behavior expected in combustion environments. The complex chemical kinetics related

to HAN and HEHN have been hardly studied. However, the first step in the decomposition mechanism for HAN and HEHN are Eqs 20 and 21, respectively: [178, 179]

$$NH_3OH^+ + NO_3^- \rightarrow NH_2OH + HNO_3 \tag{20}$$

$$HEHN \rightarrow HEH + HNO_3 \tag{21}$$

While preliminary neutral, gas–phase insights may qualitatively connect classical MD results to thermal decomposition pathways, [180–184] it is apparent that a high–throughput infrastructure will enable exploration of a wider range of concentrations and mixtures to understand what factors enhance or suppress hydrogen bonding.

Conclusions

Herein, we present the first computational high–throughput screening framework for multimode propulsion propellant discovery. The maturity of Materials Project software infrastructure and high performance computing resources presents a promising opportunity to explore ionic liquids fundamentally over a vast chemical design space. Moreover, the mixture chemistry and temperature–dependence involved with designing and characterizing macroscopic behavior of propellants adds a layer of complexity appropriate for large scale, parallelized simulations. Through the case study of [HAN][HEHN] mixtures, we show properties that inform design considerations based on molecular simulations. The goal of this work is to invite the MMP and IL community at large to generate a database of material properties to support the next–generation of IL discovery and participate in modeling and experimental efforts towards the proposed framework for propellant discovery.

Acknowledgments

This material is based upon work supported by the U.S. Department of Energy, Office of Science, Office of Advanced Scientific Computing Research, Department of Energy Computational Science Graduate Fellowship under Award Number DE–SC0022158, the NERSC ERCAP 2022 grant number ERCAP0021857, and Air Force Office of Scientific Research under Award FA9550-25-1-0012. Support on software infrastructure and data was funded by the Materials Project, which is funded by the U.S. Department of Energy, Office of Science, Office of Basic Energy Sciences, Materials Sciences and Engineering Division, under Contract no. DE-AC02-05-CH11231: Materials Project program KC23MP.

Author contributions

S. M. P.: Conceptualization (lead); Data curation (lead); Formal analysis (lead); Investigation (lead); Methodology (lead); Validation (lead); Visualization (lead); Writing – original draft (lead). Software (equal); O. A. C. & K. A. P.: Software (lead); Conceptualization (equal); Methodology (equal); Supervision (equal); G. L. V.: Methodology (equal); Project administration (equal); Supervision (equal); J. G. M.: Methodology (equal); Project administration (equal); Supervision (equal); R. E. W.: Project administration (lead); Supervision (lead); Funding acquisition (lead); Methodology (equal);

Data availability

No datasets were generated or analysed during the current study.

Declarations

Competing interests

The authors declare no competing interests.

Author details

[1]School of Chemistry and Biochemistry, Georgia Institute of Technology, Atlanta, GA 30332, USA
[2]Materials Science and Engineering, University of California, Berkeley, Berkeley, CA 94720, USA
[3]Materials Science and Engineering, Molecular Foundry and Materials Project, Faculty Staff Scientist at Lawrence Berkeley National Laboratory, Lawrence Berkeley National Laboratory, Berkeley, CA 94720, USA
[4]AFRL In-Space Propulsion Branch, Air Force Research Laboratory, Edwards AFB, CA 93524, USA
[5]Mechanical and Aerospace Engineering, University of California, Los Angeles, Los Angeles, CA 90095, USA
[6]Executive Director of Aerospace Research Programs, College of Engineering, Oregon State University, Corvallis, OR 97331, USA

Received: 1 January 2025 / Accepted: 8 December 2025

Published online: 16 January 2026

References

1. Carnero A (2006) High throughput screening in drug discovery. Clin And Transl Oncol 8(7):482–490. [Online]. Available: https://doi.org/10.1007/s12094-006-0048-2
2. Mishra KP, Ganju L, Sairam M, Banerjee PK, Sawhney RC (2008) A review of high throughput technology for the screening of natural products. Biomed Pharmacother 62(2):94–98. [Online]. Available:https://www.sciencedirect.com/science/article/pii/S0753332207001278
3. Macarron R, Banks MN, Bojanic D, Burns DJ, Cirovic DA, Garyantes T, Green DVS, Hertzberg RP, Janzen WP, Paslay JW, Schopfer U, Sittampalam GS (2011) Impact of high-throughput screening in biomedical research. Nat Rev Drug Discov 10(3):188–195. [Online]. Available: https://doi.org/10.1038/nrd3368
4. Jignesh J, Keval Y, Tejas H (2022) A brief review of high throughput screening in drug discovery process 2022. 17204 Publication Title: Current Trends in Pharmacy and Pharmaceutical Chemistry Volume: [Online]. Available:https://www.ctppc.org/article-details/17204
5. Kim JC, Moore CJ, Kang B, Hautier G, Jain A, Ceder G (2011) Synthesis and Electrochemical properties of monoclinic LiMnBO3 as a Li intercalation material. J Electrochem Soc 158(3):A309. The Electrochemical Society, Inc. [Online]. Available: https://doi.org/10.1149/1.3536532
6. Hautier G, Jain A, Chen H, Moore C, Ong SP, Ceder G (2011) Novel mixed polyanions lithium-ion battery cathode materials predicted by high-throughput ab initio computations. J Mater Chem 21(43): 17 147–17 153. The Royal Society of Chemistry. [Online]. Available:https://doi.org/10.1039/C1JM12216A
7. Chen H, Hautier G, Ceder G (2012 Dec) Synthesis, computed stability, and crystal structure of a new family of inorganic compounds: Carbonophosphates. J Am Chem Soc 134(48): 19 619–19 627. American Chemical Society. [Online]. Available: https://doi.org/10.1021/ja3040834
8. Jain A, Hautier G, Moore C, Kang B, Lee J, Chen H, Twu N, Ceder G (2012) A computational investigation of Li9M3(P2O7)3(PO4)2 (M = V, Mo) as cathodes for Li Ion Batteries. J Electrochem Soc 159(5):A622. The Electrochemical Society, Inc. [Online]. Available: https://doi.org/10.1149/2.080205jes
9. Chen H, Hautier G, Jain A, Moore C, Kang B, Doe R, Wu L, Zhu Y, Tang Y, Ceder G (2012 Jun) Carbonophosphates: a new family of cathode materials for Li-ion batteries identified computationally. Chem Of Mater 24(11):2009–2016. American Chemical Society. [Online]. Available: https://doi.org/10.1021/cm203243x
10. Alapati SV, Johnson JK, Sholl DS (2006 May) Identification of destabilized metal hydrides for hydrogen storage using first principles calculations. The J Phys Chem B 110(17):8769–8776. American Chemical Society. [Online]. Available: doi:https://doi.org/10.1021/jp060482m
11. Lu J, Fang ZZ, Choi YJ, Sohn HY (2007 Aug) Potential of binary lithium magnesium nitride for hydrogen storage applications. The J Phys Chem C 111(32): 12 129–12 134. American Chemical Society. [Online]. Available: https://doi.org/10.1021/jp0733724
12. Colón YJ, Fairen-Jimenez D, Wilmer CE, Snurr RQ (2014 Mar) High-throughput screening of porous crystalline materials for hydrogen storage capacity near room temperature. The J Phys Chem C 118(10):5383–5389. American Chemical Society. [Online]. Available: https://doi.org/10.1021/jp4122326
13. Li A, Bueno-Perez R, Madden D, Fairen-Jimenez D (2022) From computational high-throughput screenings to the lab: taking metal–organic frameworks out of the computer. Chem Sci 13(27):7990–8002. The Royal Society of Chemistry. [Online]. Available: https://doi.org/10.1039/D2SC01254E
14. Batalović K, Radaković J, Kuzmanović B, Medić Ilić M, Paskaš Mamula B (2023) Machine learning-based high-throughput screening of Mg-containing alloys for hydrogen storage and energy conversion applications. J Energy Storage 68:107720. [Online]. Available: https://www.sciencedirect.com/science/article/pii/S2352152X23011179
15. Osman AI, Nasr M, Eltaweil AS, Hosny M, Farghali M, Al-Fatesh AS, Rooney DW, El-Monaem EMA (2024) Advances in hydrogen storage materials: harnessing innovative technology, from machine learning to computational chemistry, for energy storage solutions. Int J Hydrogen Energy 67:1270–1294. [Online]. Available:https://www.sciencedirect.com/science/article/pii/S036031992401053X
16. Ahmed A, Seth S, Purewal J, Wong-Foy AG, Veenstra M, Matzger AJ, Siegel DJ (2019) Exceptional hydrogen storage achieved by screening nearly half a million metal-organic frameworks. Nat Commun 10(1):1568. [Online]. Available: https://doi.org/10.1038/s41467-019-09365-w
17. Lin L-C, Berger AH, Martin RL, Kim J, Swisher JA, Jariwala K, Rycroft CH, Bhown AS, Deem MW, Haranczyk M, Smit B (2012) In silico screening of carbon-capture materials. Nat Mater 11(7):633–641. [Online]. Available:https://doi.org/10.1038/nmat3336
18. Braun E, Zurhelle AF, Thijssen W, Schnell SK, Lin L-C, Kim J, Thompson JA, Smit B (2016) High-throughput computational screening of nanoporous adsorbents for CO2 capture from natural gas. Mol Syst Des Eng 1(2):175–188. The Royal Society of Chemistry. [Online]. Available: https://doi.org/10.1039/C6ME00043F
19. Yuan X, Deng X, Cai C, Shi Z, Liang H, Li S, Qiao Z (2021) Machine learning and high-throughput computational screening of hydrophobic metal–organic frameworks for capture of formaldehyde from air. Green Energyamp; Environ 6(5):759–770. [Online]. Available: https://www.sciencedirect.com/science/article/pii/S2468025720300972
20. Mohamed SA, Zhao D, Jiang J (2023) Integrating stability metrics with high-throughput computational screening of metal–organic frameworks for CO2 capture. Commun Mater 4(1):79. [Online]. Available: doi: https://doi.org/10.1038/s43246-023-00409-9
21. De Vos N, Maton C, Stevens CV (2014 Aug) Electrochemical stability of ionic liquids: General influences and degradation mechanisms. ChemElectrochem 1(8):1258–1270. John Wiley & Sons, Ltd. [Online]. Available: https://doi.org/10.1002/celc.201402086
22. De Vos JS, Ravichandran S, Borgmans S, Vanduyfhuys L, Voort PVD, Rogge SMJ, Van Speybroeck V (2024 May) High-throughput screening of covalent organic frameworks for carbon capture using machine learning. Chem Of Mater 36(9):4315–4330. American Chemical Society. [Online]. Available: https://doi.org/10.1021/acs.chemmater.3c03230

23. Petousis I, Mrdjenovich D, Ballouz E, Liu M, Winston D, Chen W, Graf T, Schladt TD, Persson KA, Prinz FB (2017) High-throughput screening of inorganic compounds for the discovery of novel dielectric and optical materials. Sci Data 4(1):160134. [Online]. Available: https://doi.org/10.1038/sdata.2016.134
24. "Materials Genome Initiative for Global Competitiveness," (2011) Tech. Rep
25. Council NR (2008) Integrated computational materials engineering: a transformational discipline for improved competitiveness and national security. The National Academies Press. [Online]. Available: https://nap.nationalacademies.org/catalog/12199/integrated-computational-materials-engineering-a-transformational-discipline-for-improved-competitiveness Washington, DC
26. Jain A, Ong SP, Hautier G, Chen W, Richards WD, Dacek S, Cholia S, Gunter D, Skinner D, Ceder G, Persson KA (2013 Jul) Commentary: the materials Project: a materials genome approach to accelerating materials innovation. APL Mater 1(1):011002. [Online]. Available: https://doi.org/10.1063/1.4812323
27. "National Energy Research Scientific Computing Center (2011) Annual report. Tech. Rep.," Lawrence Berkeley National Laboratory
28. Choudhary K, DeCost B, Chen C, Jain A, Tavazza F, Cohn R, Park CW, Choudhary A, Agrawal A, Billinge SJL, Holm E, Ong SP, Wolverton C (2022) Recent advances and applications of deep learning methods in materials science. Npj Comput Mater 8(1):59. [Online]. Available: https://doi.org/10.1038/s41524-022-00734-6
29. Ong SP, Richards WD, Jain A, Hautier G, Kocher M, Cholia S, Gunter D, Chevrier VL, Persson KA, Ceder G (2013) Python materials genomics (pymatgen): a robust, open-source python library for materials analysis. Comput Mater Sci 68:314–319. [Online]. Available: https://www.sciencedirect.com/science/article/pii/S0927025612006295
30. Jain A, Ong SP, Chen W, Medasani B, Qu X, Kocher M, Brafman M, Petretto G, Rignanese G-M, Hautier G, Gunter D, Persson KA (2015 Dec) FireWorks: a dynamic workflow system designed for high-throughput applications. Concurrency And Computation: Pract And Exper 27(17):5037–5059. John Wiley & Sons, Ltd. [Online]. Available: https://doi.org/10.1002/cpe.3505
31. Mathew K, Montoya JH, Faghaninia A, Dwarakanath S, Aykol M, Tang H, Chu I-H, Smidt T, Bocklund B, Horton M, Dagdelen J, Wood B, Liu Z-K, Neaton J, Ong SP, Persson K, Jain A (2017) Atomate: a high-level interface to generate, execute, and analyze computational materials science workflows. Comput Mater Sci 139:140–152. [Online]. Available: https://www.sciencedirect.com/science/article/pii/S0927025617303919
32. Haase FT, Bergmann A, Jones TE, Timoshenko J, Herzog A, Jeon HS, Rettenmaier C, Cuenya BR (2022) Size effects and active state formation of cobalt oxide nanoparticles during the oxygen evolution reaction. Nat Energy 7(8):765–773. [Online]. Available: https://doi.org/10.1038/s41560-022-01083-w
33. Ko Y-J, Kim J-Y, Lee WH, Kim MG, Seong T-Y, Park J, Jeong Y, Min BK, Lee W-S, Lee DK, Oh H-S (2022) Exploring dopant effects in stannic oxide nanoparticles for CO2 electro-reduction to formate. Nat Commun 13(1):2205. [Online]. Available:https://doi.org/10.1038/s41467-022-29783-7
34. Price TW, Evans DD (1968) The status of monopropellant hydrazine technology. Tech. Rep. [Online]. Available:https://ntrs.nasa.gov/citations/19680006875 Jet Propulsion Laboratory, California Institute of Technology, Pasadena, California
35. Wood SE, Bryant JT (1973 Jun) Decomposition of hydrazine on Shell 405 catalyst at high presure. Prod R&D 12(2):117–122. American Chemical Society. [Online]. Available: https://doi.org/10.1021/i360046a004
36. Schmidt MW, Gordon MS (2013) The decomposition of hydrazine in the gas phase and over an iridium catalyst 227(11):1301–1336. [Online]. Available: https://doi.org/10.1524/zpch.2013.0404
37. Wirz R, Mueller J, Gale M, Marrese C (2004 Jul) Miniature ion thruster for precision formation flying. In 40th AIAA/ASME/SAE/ASEE Joint Propulsion Conference and Exhibit, American Institute of Aeronautics and Astronautics. series Title: Joint Propulsion Conferences. [Online] Available: https://doi.org/10.2514/6.2004-4115
38. Goebel DM, Katz I (2008) Fundamentals of electric propulsion: ion and hall thrusters. Jet Propulsion Laboratory, California Institute of Technology
39. Rovey JL, Lyne CT, Mundahl AJ, Rasmont N, Glascock MS, Wainwright MJ, Berg SP (2020 Oct) Review of multimode space propulsion. Prog In Aerosp Sci 118:100627. [Online]. Available: https://www.sciencedirect.com/science/article/pii/S0376042120300397
40. Hori K, Katsumi T, Sawai S, Azuma N, Hatai K, Nakatsuka J (2019 Sep) HAN-Based Green propellant, SHP163 – its R&D and Test in space. Propellants, Explos, Pyrotech 44(9):1080–1083. John Wiley & Sons, Ltd. [Online]. Available: https://doi.org/10.1002/prep.201900237
41. McLean CH (2020 Aug) Green propellant infusion mission: program construct, technology development, and mission results. In: AIAA propulsion and energy 2020 forum. American Institute of Aeronautics and Astronautics. series Title: AIAA Propulsion and Energy Forum. [Online]. Available: https://doi.org/10.2514/6.2020-3810
42. Ziemer JK, Marrese-Reading C, Arestie SM, Conroy DG, Leifer SD, Ortega AL, Demmons NR, Wirz RE, Gamero M Incorporating lessons learned into LISA colloid microthruster technology development. In: AIAA propulsion and energy 2019 forum. American Institute of Aeronautics and Astronautics, series Title: AIAA Propulsion and Energy Forum
43. Ye C, Liu W, Chen Y, Yu L (2001) Room-temperature ionic liquids: a novel versatile lubricant. Chem Commun (21):2244–2245. The Royal Society of Chemistry. [Online]. Available: https://doi.org/10.1039/B106935G
44. Tokuda H, Hayamizu K, Ishii K, Susan MABH, Watanabe M (2005 Apr) Physicochemical properties and structures of room temperature ionic liquids. 2. Variation of alkyl chain length in imidazolium cation. The J Phys Chem B 109(13):6103–6110. American Chemical Society. [Online]. Available: https://doi.org/10.1021/jp044626d
45. Galiński M, Lewandowski A, Stępniak I (2006 Aug) Ionic liquids as electrolytes. Electrochim Acta 51(26):5567–5580. [Online]. Available: https://www.sciencedirect.com/science/article/pii/S0013468606002362
46. Sam II, Gayathri S, Santhosh G, Cyriac J, Reshmi S (2022 Mar) Exploring the possibilities of energetic ionic liquids as non-toxic hypergolic bipropellants in liquid rocket engines. J Mol Liq 350:118217. [Online]. Available: https://www.sciencedirect.com/science/article/pii/S0167732221029421
47. Navarra MA (2013) Ionic liquids as safe electrolyte components for Li-metal and Li-ion batteries. MRS Bull 38(7):548–553. Cambridge University Press. [Online]. Available: https://www.cambridge.org/core/article/ionic-liquids-as-safe-electrolyte-components-for-limetal-and-liion-batteries/BF2188216342E55B75CF661EBFFC9F1F
48. MacFarlane DR, Tachikawa N, Forsyth M, Pringle JM, Howlett PC, Elliott GD, Davis JH, Watanabe M, Simon P, Angell CA (2014) Energy applications of ionic liquids. Energy Environ Sci 7(1):232–250. The Royal Society of Chemistry. [Online]. Available: https://doi.org/10.1039/C3EE42099J

49. Watanabe M, Thomas ML, Zhang S, Ueno K, Yasuda T, Dokko K (2017 May) Application of ionic liquids to Energy storage and conversion materials and devices. Chem Rev 117(10):7190–7239. American Chemical Society. [Online]. Available: https://doi.org/10.1021/acs.chemrev.6b00504
50. Balducci A (2017) Ionic liquids in lithium-ion batteries. Top In Curr Chem 375(2):20. [Online]. Available: https://doi.org/10.1007/s41061-017-0109-8
51. Haddad AZ, Menon AK, Kang H, Urban JJ, Prasher RS, Kostecki R (2021 Mar) Solar desalination using thermally responsive ionic liquids regenerated with a photonic Heater. Environ Sci Technol 55(5):3260–3269. American Chemical Society. [Online]. Available: https://doi.org/10.1021/acs.est.0c06232
52. Gurkan BE, de la Fuente JC, Mindrup EM, Ficke LE, Goodrich BF, Price EA, Schneider WF, Brennecke JF (2010 Feb) Equimolar CO2 absorption by anion-functionalized ionic liquids. J Am Chem Soc 132(7):2116–2117. American Chemical Society. [Online]. Available: https://doi.org/10.1021/ja909305t
53. Berg SP, Rovey JL (2013) Assessment of high-power electric multi-mode Spacecraft propulsion concepts. . [Online]. Available: https://api.semanticscholar.org/CorpusID:8942140
54. Berg SP, Rovey JL (2017 Mar) Assessment of multimode Spacecraft micropropulsion systems. J Spacecraft And Rockets 54(3):592–601. American Institute of Aeronautics and Astronautics. [Online]. Available: https://doi.org/10.2514/1.A33649
55. Donius B, Rovey J (2010) Analysis and prediction of dual-mode Chemical and electric ionic liquid propulsion performance. In: 48th AIAA aerospace sciences meeting including the New horizons Forum and aerospace exposition. American Institute of Aeronautics and Astronautics, series Title: Aerospace Sciences Meetings. [Online]. Jan]. Available: https://doi.org/10.2514/6.2010-1328
56. Donius BR, Rovey JL (2011 Jan) Ionic liquid dual-mode Spacecraft propulsion Assessment. J Spacecraft And Rockets 48(1):110–123. American Institute of Aeronautics and Astronautics. [Online]. Available: https://doi.org/10.2514/1.49959
57. Oh DY, Randolph T, Kimbrel S, Martinez-Sanchez M (2004 Sep) End-to-end optimization of Chemical-electric orbit-raising missions. J Spacecraft And Rockets 41(5):831–839. American Institute of Aeronautics and Astronautics. [Online]. Available: https://doi.org/10.2514/1.13096
58. Kluever CA (2012 Nov) Optimal geostationary orbit transfers using onboard Chemical-electric propulsion. J Spacecraft And Rockets 49(6):1174–1182. American Institute of Aeronautics and Astronautics. [Online]. Available: https://doi.org/10.2514/1.A32213
59. Kuo K "Principles of combustion 3rd Edition Wiley." [Online]. Available: https://www.wiley.com/en-us/Principles+of+Combustion%2C+3rd+Edition-p-9781394187072
60. Mora JFDL, Loscertales IG (1994) The current emitted by highly conducting Taylor cones. J Fluid Mech 260:155–184. Cambridge University Press. [Online]. Available: https://www.cambridge.org/core/article/current-emitted-by-highly-conducting-taylor-cones/B47A42612F7D0FBA970319CFFA0DCADD
61. Gamero-Castaño M, Fernández de la Mora J (2000 Jun) Direct measurement of ion evaporation kinetics from electrified liquid surfaces. The J Chem Phys 113(2):815–832. American Institute of Physics. [Online]. Available: https://doi.org/10.1063/1.481857
62. Romero-Sanz I, Bocanegra R, Fernandez de la Mora J, Gamero-Castaño M (2003 Aug) Source of heavy molecular ions based on Taylor cones of ionic liquids operating in the pure ion evaporation regime. J Appl Phys 94(5):3599–3605. American Institute of Physics. [Online]. Available: https://doi.org/10.1063/1.1598281
63. Lozano PC (2005) Energy properties of an EMI-Im ionic liquid ion source. J Phys D: Appl Phys 39(1):126–134. IOP Publishing. [Online]. Available: https://doi.org/10.1088/0022-3727/39/1/020
64. Sackheim RL (2003 Jan) Spacecraft Chemical propulsion. In: Meyers RA (ed) Encyclopedia of physical science and technology, *Third Edition)* edn. Academic Press, New York, pp 403–430. [Online]. Available: https://www.sciencedirect.com/science/article/pii/B0122274105009042
65. Sutton GP, Biblarz O Rocket Propulsion Elements
66. Gordon S, Mcbride BJ (1994 Oct) Computer program for calculation of complex chemical equilibrium compositions and applications. Part 1: analysis,". nTRS Author Affiliations: NASA Lewis Research Center NTRS Report/Patent Number: NAS 1.61:1311 NTRS Document ID: 19950013764 NTRS Research Center: Legacy CDMS (CDMS). [Online]. Available: https://ntrs.nasa.gov/citations/19950013764
67. Wagman DD (1982) The NBS tables of chemical thermodynamic properties: selected values for inorganic and C_1 and C_2 organic substances in si units. In: Ser. Journal of physical and chemical reference data., vol oCLC. American Chemical Society and the American Institute of Physics for the National Bureau of Standards, Washington, DC, p 9622610
68. Denbigh KG (1981) The principles of chemical equilibrium: with applications in chemistry and chemical engineering. Cambridge University Press 4th ed. Cambridge. [Online]. Available: https://www.cambridge.org/core/books/principles-of-chemical-equilibrium/3BAF3584DF52BE826808D091F3B0E4E5,
69. Beattie JA (1956 Jun) The principles of Chemical equilibrium, with applications in Chemistry and Chemical engineering. J Am Chem Soc 78(12):2916–2916. [Online]. Available: https://pubs.acs.org/doi/abs/10.1021/ja01593a082
70. Benson SW, Cruickshank FR, Golden DM, Haugen GR, O'Neal HE, Rodgers AS, Shaw R, Walsh R (1969 Jun) Additivity rules for the estimation of thermochemical properties. Chem Rev 69(3):279–324. American Chemical Society. [Online]. Available: https://doi.org/10.1021/cr60259a002
71. McMillen DF, Golden DM (1982 Oct) Hydrocarbon bond dissociation energies. Annu Rev Phys Chem 33(1):493–532. [Online]. Available: https://www.annualreviews.org/doi/10.1146/annurev.pc.33.100182.002425
72. Domalski ES, Hearing ED (1996 Jan) Heat capacities and entropies of organic compounds in the condensed phase. Volume iii. J Phys And Chem Reference Data 25(1):1. [Online]. Available: https://doi.org/10.1063/1.555985
73. Kobrak MN, Sandalow N (2004 Jan) An electrostatic interpretation of structure-property relationships in ionic liquids," ECS Proceedings Volumes, vol. 2004-24(1):417. IOP Publishing. [Online]. Available: https://iopscience.iop.org/article/10.1149/200424.0417PV/meta
74. Gharagheizi F, Sattari M, Ilani-Kashkouli P, Mohammadi AH, Ramjugernath D, Richon D (2013 Sep) A "non-linear" quantitative structure–property relationship for the prediction of electrical conductivity of ionic liquids. Chem Eng Sci 101:478–485. [Online]. Available: https://www.sciencedirect.com/science/article/pii/S0009250913004983
75. Greaves TL, Drummond CJ (2015 Oct) Protic ionic liquids: evolving structure–property relationships and expanding applications. Chem Rev 115(20): 11 379–11 448. American Chemical Society. [Online]. Available: doi: https://doi.org/10.1021/acs.chemrev.5b00158

76. Silva W, Zanatta M, Ferreira AS, Corvo MC, Cabrita EJ (2020 Jan) Revisiting ionic liquid structure-property relationship: a critical analysis. Int J Mol Sci 21(20):7745. Multidisciplinary Digital Publishing Institute. [Online]. Available: https://www.mdpi.com/1422-0067/21/20/7745
77. Duong DV, Tran H-V, Pathirannahalage SK, Brown SJ, Hassett M, Yalcin D, Meftahi N, Christofferson AJ, Greaves TL, Le TC (2022 Apr) Machine learning investigation of viscosity and ionic conductivity of protic ionic liquids in water mixtures. The J Chem Phys 156(15):154503. [Online]. Available: https://doi.org/10.1063/5.0085592
78. Toots KM, Sild S, Leis J, Acree WE, Maran U (2022 Jul) Machine learning quantitative structure-property relationships as a function of ionic liquid cations for the gas-ionic liquid partition coefficient of hydrocarbons. Int J Mol Sci 23(14):7534
79. Bejaoui YKJ, Philippi F, Stammler H-G, Radacki K, Zapf L, Schopper N, Goloviznina K, Maibom KAM, Graf R, Sprenger JAP, Bertermann R, Braunschweig H, Welton T, Ignat'ev NV, Finze M (2023 Feb) Insights into structure–property relationships in ionic liquids using cyclic perfluoroalkylsulfonylimides. Chem Sci 14(8):2200–2214. The Royal Society of Chemistry. [Online]. Available: https://pubs.rsc.org/en/content/articlelanding/2023/sc/d2sc06758g
80. Esteva FJC, Zhang Y, Roman ASA, Maginn EJ, Colón YJ (2025 Jul) Structure-property relationship for the electrostrictive properties of ionic liquids. The J Phys Chem. B 129(28):7293–7300
81. Newsome DA, Vaghjiani GL, Chambreau SD, Yos D, Wolf MJ, Sengupta D (2025 Jul) Development of linear structure property relationship for energetic materials using machine learning. J Mol Liq 429:127480. [Online]. Available: https://www.sciencedirect.com/science/article/pii/S0167732225006476
82. Thorat A, Verma AK, Chauhan R, Sartape R, Singh MR, Shah JK (2025 Feb) Identifying high ionic conductivity compositions of ionic liquid electrolytes using features of the solvation environment. J Chem Theory Computation 21(4):1929–1940. American Chemical Society. [Online]. Available: https://doi.org/10.1021/acs.jctc.4c01441
83. McDaniel JG, Choi E, Son CY, Schmidt JR, Yethiraj A (2016 Jul) Ab initio force fields for imidazolium-based ionic liquids. The J Phys Chem B 120(28):7024–7036. American Chemical Society. [Online]. Available: https://doi.org/10.1021/acs.jpcb.6b05328
84. McDaniel JG, Son CY (2018 Jul) Ion correlation and collective dynamics in BMIM/BF4-based organic electrolytes: from dilute solutions to the ionic liquid limit. The J Phys Chem B 122(28):7154–7169. American Chemical Society. [Online]. Available: https://doi.org/10.1021/acs.jpcb.8b04886
85. Kandil ME, Marsh KN, Goodwin ARH (2007 Nov) Measurement of the viscosity, density, and electrical conductivity of 1-hexyl-3-methylimidazolium Bis(trifluorosulfonyl)imide at temperatures between (288 and 433) K and Pressures below 50 MPa. J Chem Eng Data 52(6):2382–2387. American Chemical Society. [Online]. Available: https://doi.org/10.1021/je7003484
86. Kubisiak P, Eilmes A (2020 Oct) Estimates of electrical conductivity from molecular dynamics simulations: how to invest the computational effort. The J Phys Chem B 124(43):9680–9689. American Chemical Society. [Online]. Available: https://doi.org/10.1021/acs.jpcb.0c07704
87. Verma AK, Thorat AS, Shah JK (2024 Jun) Estimating ionic conductivity of ionic liquids: nernst–Einstein and Einstein formalisms. J Ionic Liq 4(1):100089. [Online]. Available: https://www.sciencedirect.com/science/article/pii/S2772422024000120
88. "1-Butyl-3-methylimidazolium tetrafluoroborate, >99% IoLiTec." [Online]. Available: https://iolitec.de/en/products/ionic_liquids/catalogue/imidazolium-based/il-0012-hp
89. "1-Ethyl-3-methylimidazolium bis(trifluoromethylsulfonyl)imide, >99.5% IoLiTec." [Online]. Available: https://iolitec.de/en/node/455
90. "1-Hexyl-3-methylimidazolium tetrafluoroborate, >99% IoLiTec." [Online]. Available: https://iolitec.de/en/node/123
91. Xu W-G, Li L, Ma X-X, Wei J, Duan W-B, Guan W, Yang J-Z (2012 Aug) Density, surface tension, and refractive index of ionic liquids homologue of 1-alkyl-3-methylimidazolium tetrafluoroborate [Cnmim][BF4] (n = 2,3,4,5,6). J Chem Eng Data 57(8):2177–2184. American Chemical Society. [Online]. Available: https://doi.org/10.1021/je3000348
92. Goddu B, Tadavarthi MM, Tadekoru VK, Guntupalli JN (2019 Jun) Density, speed of sound, and dynamic viscosity of 1-Butyl-3-methylimidazolium Bis(trifluoromethylsulfonyl)imide/1-Butyl-3-methylimidazolium hexafluorophosphate and N-Methylaniline binary systems from T = 298.15 to 323.15 K at 0.1 MPa. J Chem Eng Data 64(6):2303–2319. American Chemical Society. [Online]. Available: https://doi.org/10.1021/acs.jced.8b01095
93. Carvalho PJ, Freire MG, Marrucho IM, Queimada AJ, Coutinho JAP (2008 Jun) Surface tensions for the 1-alkyl-3-methylimidazolium Bis(trifluoromethylsulfonyl)imide ionic liquids. J Chem Eng Data 53(6):1346–1350. [Online]. Available: https://pubs.acs.org/doi/10.1021/je800069z
94. Fröba AP, Kremer H, Leipertz A (2008 Oct) "Density, Refractive Index, Interfacial Tension, and Viscosity of Ionic Liquids [EMIM][EtSO4], [EMIM][NTf2], [EMIM][N(CN)2], and [OMA][NTf2] in Dependence on Temperature at Atmospheric Pressure,". The J Phys Chem B 112(39): 12 420–12 430. American Chemical Society. [Online]. Available: doi:https://doi.org/10.1021/jp804319a
95. Ghatee MH, Zolghadr AR (2008 Feb) Surface tension measurements of imidazolium-based ionic liquids at liquid–vapor equilibrium. Fluid Phase Equilib 263(2):168–175. [Online]. Available: https://www.sciencedirect.com/science/article/pii/S0378381207006383
96. Sánchez LG, Espel JR, Onink F, Meindersma GW, Haan ABD (2009 Oct) Density, viscosity, and surface tension of Synthesis grade imidazolium, pyridinium, and pyrrolidinium based room temperature ionic liquids. J Chem Eng Data 54(10):2803–2812. American Chemical Society. [Online]. Available: https://doi.org/10.1021/je800710p
97. Součková M, Klomfar J, Pátek J (2011 Apr) Surface tension of 1-alkyl-3-methylimidazolium based ionic liquids with trifluoromethanesulfonate and tetrafluoroborate anion. Fluid Phase Equilib 303(2):184–190. . [Online]. Available: https://www.sciencedirect.com/science/article/pii/S0378381211000549
98. "1-Butyl-3-methylimidazolium bis(trifluoromethylsulfonyl)imide, >99.5% IoLiTec." [Online]. Available: https://iolitec.de/en/node/456
99. Tamayol A, Bahrami M (2011 Apr) Transverse permeability of fibrous porous media. Phys Rev E 83(4):046314. [Online]. Available: https://link.aps.org/doi/10.1103/PhysRevE.83.046314
100. Schreiner C, Zugmann S, Hartl R, Gores HJ (2010 May) Fractional walden rule for ionic liquids: examples from recent measurements and a critique of the So-called ideal KCl line for the walden plot. J Chem Eng Data 55(5):1784–1788. American Chemical Society. [Online]. Available: https://doi.org/10.1021/je900878j

101. Villegas-Prados D, Cruz J, Wijnen M, Fajardo P, Navarro-Cavallé J (2024 Jun) Emission and performance characterization of ionic liquids for an externally wetted electrospray thruster. Acta Astronautica 219:97–107. . [Online]. Available: https://www.sciencedirect.com/science/article/pii/S0094576524001334
102. Fonda-Marsland E, Ryan C (2017 Jul) Preliminary ionic liquid propellant selection for dual-mode Micro-propulsion systems. In 53rd AIAA/SAE/ASEE Joint Propulsion Conference, American Institute of Aeronautics and Astronautics, series Title: AIAA Propulsion and Energy Forum. [Online]. Available: https://doi.org/10.2514/6.2017-5019
103. Hawkins T (2005) "Research and development of ionic liquids at U.S. Air force Research Laboratory ionic liquids R&D – U.S. Air force Research Laboratory," Project No. 5026, Task No. 0541, Tech. Rep. Air Force Research Laboratory, Edwards Air Force Base, CA
104. Gao A, Oyumi Y, Brill TB (1991) Thermal decomposition of energetic materials 49. Thermolysis routes of mono- and diaminotetrazoles. Combust And Flame 83(3):345–352. [Online]. Available: https://www.sciencedirect.com/science/article/pii/0010218091900081L
105. Lesnikovich AI, Ivashkevich OA, Levchik SV, Balabanovich AI, Gaponik PN, Kulak AA (2002) Thermal decomposition of aminotetrazoles. Thermochim Acta 388(1):233–251. [Online]. Available: https://www.sciencedirect.com/science/article/pii/S0040603102000278
106. Schneider S, Hawkins T, Rosander M, Vaghjiani G, Chambreau S, Drake G (2008 Jul) Ionic liquids as hypergolic fuels. Energy Fuels 22(4):2871–2872. American Chemical Society. [Online]. Available: https://doi.org/10.1021/ef800286b
107. Lin Q-H, Li Y-C, Li Y-Y, Wang Z, Liu W, Qi C, Pang S-P (2012) Energetic salts based on 1-amino-1,2,3-triazole and 3-methyl-1-amino-1,2,3-triazole. J Mater Chem 22(2):666–674. The Royal Society of Chemistry. [Online]. Available: https://doi.org/10.1039/C1JM14322K
108. Zhang Y, Gao H, Guo Y, Joo Y-H, Shreeve JM (2010 Mar) Hypergolic N,N-Dimethylhydrazinium ionic liquids. Chem – A Eur J 16(10):3114–3120. John Wiley & Sons, Ltd. [Online]. Available: https://doi.org/10.1002/chem.200902725
109. Smiglak M, Hines CC, Wilson TB, Singh S, Vincek AS, Kirichenko K, Katritzky AR, Rogers RD (2010 Feb) Ionic liquids based on azolate anions. Chem – A Eur J 16(5):1572–1584. John Wiley & Sons, Ltd. [Online]. Available: https://doi.org/10.1002/chem.200901418
110. Joo Y-H, Gao H, Zhang Y, Shreeve JM (2010 Apr) Inorganic or organic Azide-containing hypergolic ionic liquids as poster published in 1st Korean International symposium on high Energy materials, Incheon, Korea, October 6-9, 2009. Inorg Chem 49(7):3282–3288, American Chemical Society. [Online]. Available: https://doi.org/10.1021/ic902224t
111. Habereder T, Hammerl A, Holl G, Klapötke TM, Knizek J, Nöth H (1999 May) Synthesis and X-ray structure determination of tert-Butylhydrazinium Azide and N,N,N-Trimethylhydrazinium Azide. Eur J Inorg Chem 1999(5):849–852. John Wiley & Sons, Ltd. [Online]. Available: https://doi.org/10.1002/(SICI)1099-0682(199905)1999:5%3C849::AID-EJIC849%3E3.0.CO
112. Hammerl A, Holl G, Kaiser M, Klapötke TM, Mayer P, Nöth H, Warchhold M (2001 Jul) New hydrazinium azide compounds. Z für Anorg und Allg Chem 627(7):1477–1482. John Wiley & Sons, Ltd. [Online]. Available: https://doi.org/10.1002/1521-3749(200107)627:7%3C1477::AID-ZAAC1477%3E3.0.CO
113. Hammerl A, Holl G, Kaiser M, Klapötke TM, Kränzle R, Vogt M (2002 Jan) N,N'-Diorganylsubstituted Hydrazinium Azides. Z für Anorg und Allg Chem 628(1):322–325. John Wiley & Sons, Ltd. [Online]. Available: https://doi.org/10.1002/1521-3749(200201)628:1%3C322::AID-ZAAC322%3E3.0.CO
114. Schneider S, Hawkins T, Rosander M, Mills J, Vaghjiani G, Chambreau S (2008 Jul) Liquid azide salts and their reactions with common oxidizers IRFNA and N2O4. Inorg Chem 47(13):6082–6089. American Chemical Society. [Online]. Available: https://doi.org/10.1021/ic8004739
115. Wilhelm M, Negri M, Ciezki H, Schlechtriem S (2019) Preliminary tests on thermal ignition of ADN-based liquid monopropellants. Acta Astronautica 158:388–396. [Online]. Available: https://www.sciencedirect.com/science/article/pii/S0094576518301152
116. Persson M, Anflo K, Friedhoff P (2019 Sep) Flight heritage of ammonium dinitramide (ADN) based high performance Green propulsion (HPGP) systems. Propellants, Explos, Pyrotech 44(9):1073–1079. John Wiley & Sons, Ltd. [Online]. Available: https://doi.org/10.1002/prep.201900248
117. Masse R, Overly J, Allen M, Spores R (2012 Jul) A new state-of-the-art in AF-M315E thruster technologies. In 48th AIAA/ASME/SAE/ASEE Joint Propulsion Conference & Exhibit. American Institute of Aeronautics and Astronautics, series Title: Joint Propulsion Conferences. [Online]. Available: https://doi.org/10.2514/6.2012-4335
118. Miller CE, Lozano PC (2020 Jun) Measurement of the dissociation rates of ion clusters in ionic liquid ion sources. Appl Phys Lett 116(25):254101. American Institute of Physics. [Online]. Available: https://doi.org/10.1063/5.0006529
119. Gamero-Castaño M (2008 Mar) Characterization of the electrosprays of 1-ethyl-3-methylimidazolium bis(trifluoromethylsulfonyl) imide in vacuum. Phys Of Fluids 20(3):32103. American Institute of Physics. [Online]. Available: https://doi.org/10.1063/1.2899658
120. Prince BD, Annesley CJ, Bemish R, Hunt S (2019 Aug) Solvated ion cluster dissociation rates for ionic liquid electrospray propellants. In: AIAA propulsion and energy 2019 forum. American Institute of Aeronautics and Astronautics. , series Title: AIAA Propulsion and Energy Forum. [Online]. Available: https://doi.org/10.2514/6.2019-4170
121. Berg SP, Rovey J (2016 Jul) Decomposition of a double salt ionic liquid monopropellant on heated metallic surfaces. In 52nd AIAA/SAE/ASEE Joint Propulsion Conference, American Institute of Aeronautics and Astronautics , series Title: AIAA Propulsion and Energy Forum. [Online]. Available: https://doi.org/10.2514/6.2016-4578
122. Mundahl AJ, Berg SP, Rovey J, Huang M, Woelk K, Wagle D, Baker G (2017 Jul) Characterization of a novel ionic liquid monopropellant for multi-mode propulsion. In 53rd AIAA/SAE/ASEE Joint Propulsion Conference, American Institute of Aeronautics and Astronautics: AIAA Propulsion and Energy Forum, series Title. [Online]. Available: doi: https://doi.org/10.2514/6.2017-4756
123. Wainwright MJ, Rovey JL, Miller SW, Prince BD, Berg SP (2019 Jun) Hydroxylammonium nitrate species in a monopropellant electrospray plume. J Propul And Power 35(5):922–929. American Institute of Aeronautics and Astronautics. [Online]. Available: https://doi.org/10.2514/1.B37471
124. Thrasher J, Williams S, Takahashi P, Sousa J (2016 Jul) Pulsed plasma thruster development using a novel HAN-Based Green electric monopropellant. In 52nd AIAA/SAE/ASEE Joint Propulsion Conference, American Institute of Aeronautics and Astronautics: AIAA Propulsion and Energy Forum, series Title. [Online]. Available: https://doi.org/10.2514/6.2016-4846

125. Masse RK, Spores R, Allen M (2020 Aug) AF-M315E advanced Green propulsion ? GPIM and Beyond. In: *AIAA propulsion and energy 2020 Forum*, ser. AIAA propulsion and energy forum. American Institute of Aeronautics and Astronautics. [Online]. Available: https://arc.aiaa.org/doi/10.2514/6.2020-3517
126. Kohno Y, Ohno H (2012) Temperature-responsive ionic liquid/water interfaces: relation between hydrophilicity of ions and dynamic phase change. Phys Chem Chem Phys 14(15):5063–5070. The Royal Society of Chemistry. [Online]. Available: https://doi.org/10.1039/C2CP24026B
127. Chatel G, Pereira JFB, Debbeti V, Wang H, Rogers RD (2014) Mixing ionic liquids – "simple mixtures" or "double salts"? Green Chem 16(4):2051–2083. The Royal Society of Chemistry. [Online]. Available: https://doi.org/10.1039/C3GC41389F
128. Jorgensen WL, Maxwell DS, Tirado-Rives J (1996 Nov) Development and testing of the OPLS all-atom force field on conformational energetics and properties of organic liquids. J Am Chem Soc 118(45): 11 225–11 236. American Chemical Society. [Online]. Available: https://doi.org/10.1021/ja9621760
129. Spoel DVD, Lindahl E, Hess B, Groenhof G, Mark AE, Berendsen HJC (2005 Dec) "GROMACS: fast, flexible, and free." source+. J Comput Chem 26(16):1701–1718, place: United States
130. Wang Y, Fass J, Chodera JD (2020) End-to-end differentiable molecular mechanics force field construction. ArXiv abs/2010
131. Borodin O (2009 Aug) Polarizable force field development and molecular dynamics simulations of ionic liquids. The J Phys Chem B 113(33): 11 463–11 478. American Chemical Society. [Online]. Available: https://doi.org/10.1021/jp905220k
132. Goloviznina K, Gong Z, Padua AAH (2022 May) The CL&Pol polarizable force field for the simulation of ionic liquids and eutectic solvents. WIREs Comput Mol Sci 12(3):e1572. John Wiley & Sons, Ltd. [Online]. Available: https://doi.org/10.1002/wcms.1572
133. Goloviznina K, Gong Z, Gomes MFC, Pádua AAH (2021 Mar) Extension of the CL&Pol polarizable force field to electrolytes, protic ionic liquids, and deep eutectic solvents. J Chem Theory Computation 17(3):1606–1617. American Chemical Society. [Online]. Available: https://doi.org/10.1021/acs.jctc.0c01002
134. Bedrov D, Piquemal JP, Borodin O, MacKerell AD, Roux B, Schröder C (2019 Jul) Molecular dynamics simulations of ionic liquids and electrolytes using polarizable force fields. Chem Rev 119(13):7940–7995. American Chemical Society. [Online]. Available: https://pubs.acs.org/sharingguidelines
135. Hansen J-P, McDonald IRBT (2013) Theory of simple liquids. Academic Press. [Online]. Available: https://www.sciencedirect.com/science/article/pii/B9780123870322000131 Oxford, U.K
136. Hansen JP, McDonald IR (1975 Jun) Statistical mechanics of dense ionized matter. IV. Density and charge fluctuations in a simple molten salt. Phys Rev A 11(6):2111–2123. American Physical Society. [Online]. Available: https://link.aps.org/doi/10.1103/PhysRevA.11.2111
137. Caillol JM (1987 Jul) The dielectric constant and the conductivity of an electrolyte solution at finite wave-lengths and frequencies. Europhys Lett 4(2):159. [Online]. Available: https://doi.org/10.1209/0295-5075/4/2/006
138. Martin PA (1988) Sum rules in charged fluids. Rev Of Mod Phys 60(4):1075–1127
139. H. F, Stillinger Jr., Lovett R (1968 Sep) General restriction on the distribution of ions in electrolytes. The J Chem Phys 49(5):1991–1994. [Online]. Available: https://doi.org/10.1063/1.1670358
140. McDaniel JG, Yethiraj A (2018 Aug) Influence of electronic polarization on the structure of ionic liquids. The J Phys Chem Lett 9(16):4765–4770. American Chemical Society. [Online]. Available: https://doi.org/10.1021/acs.jpclett.8b02120
141. McDaniel JG, Yethiraj A (2019 Apr) Understanding the properties of ionic liquids: electrostatics, structure factors, and their sum rules. The J Phys Chem B 123(16):3499–3512. American Chemical Society. [Online]. Available: https://doi.org/10.1021/acs.jpcb.9b00963
142. Martínez L, Andrade R, Birgin EG, Martínez JM (2009 Oct) PACKMOL: a package for building initial configurations for molecular dynamics simulations. J Comput Chem 30(13):2157–2164. John Wiley & Sons, Ltd. [Online]. Available: https://doi.org/10.1002/jcc.21224
143. Ganose AM, Sahasrabuddhe H, Asta M, Beck K, Biswas T, Bonkowski A, Bustamante J, Chen X, Chiang Y, Chrzan DC, Clary J, Cohen OA, Ertural C, Gallant MC, George J, Gerits S, Goodall REA, Guha RD, Hautier G, Horton M, Inizan TJ, Kaplan AD, Kingsbury RS, Kuner MC, Li B, Linn X, McDermott MJ, Mohanakrishnan RS, Naik AN, Neaton JB, Parmar SM, Persson KA, Petretto G, Purcell TAR, Ricci F, Rich B, Riebesell J, Rignanese G-M, Rosen AS, Scheffler M et al. (2025 Jul) Atomate2: modular workflows for materials science. Digital discovery. RSC. [Online]. Available: https://pubs.rsc.org/en/content/articlelanding/2025/dd/d5dd00019j, publisher
144. Mobley DL, Bannan CC, Rizzi A, Bayly CI, Chodera JD, Lim VT, Lim NM, Beauchamp KA, Slochower DR, Shirts MR, Gilson MK, Eastman PK (2018 Nov) Escaping atom types in force fields using direct Chemical perception. J Chem Theory Computation 14(11):6076–6092. American Chemical Society. [Online]. Available: https://doi.org/10.1021/acs.jctc.8b00640
145. Weininger D (1988 Feb) Smiles, a chemical language and information system. 1. Introduction to methodology and encoding rules. J Chem Inf And Comput Sci 28(1):31–36. American Chemical Society. [Online]. Available: https://doi.org/10.1021/ci00057a005
146. Wang L, Behara PK, Thompson MW, Gokey T, Wang Y, Wagner JR, Cole DJ, Gilson MK, Shirts MR, Mobley DL (2024 Jul) The Open force field Initiative: Open software and Open science for molecular modeling. The J Phys Chem B 128(29):7043–7067. American Chemical Society. [Online]. Available: https://doi.org/10.1021/acs.jpcb.4c01558
147. Qiu Y, Smith DGA, Boothroyd S, Jang H, Hahn DF, Wagner J, Bannan CC, Gokey T, Lim VT, Stern CD, Rizzi A, Tjanaka B, Tresadern G, Lucas X, Shirts MR, Gilson MK, Chodera JD, Bayly CI, Mobley DL, Wang L-P (2021 Oct) Development and benchmarking of Open force field v1.0.0—the parsley small-molecule force field. J Chem Theory Computation 17(10):6262–6280. American Chemical Society. [Online]. Available: https://doi.org/10.1021/acs.jctc.1c00571
148. Eastman P, Swails J, Chodera JD, McGibbon RT, Zhao Y, Beauchamp KA, Wang L-P, Simmonett AC, Harrigan MP, Stern CD, Wiewiora RP, Brooks BR, Pande VS (2017 Jul) OpenMM 7: rapid development of high performance algorithms for molecular dynamics. PLoS Comput Biol 13(7):e1005659. Public Library of Science. [Online]. Available: https://doi.org/10.1371/journal.pcbi.1005659
149. Michaud-Agrawal N, Denning EJ, Woolf TB, Beckstein O (2011 Jul) Mdanalysis: a toolkit for the analysis of molecular dynamics simulations. J Comput Chem 32(10):2319–2327. John Wiley & Sons, Ltd. [Online]. Available: https://doi.org/10.1002/jcc.21787
150. Cohen OA, Macdermott-Opeskin H, Lee L, Hou T, Fong KD, Kingsbury R, Wang J, Persson KA (2023) SolvationAnalysis: a Python toolkit for understanding liquid solvation structure in classical molecular dynamics simulations. J Open Source Softw 8(84):5183

151. Hayes R, Imberti S, Warr GG, Atkin R (2013 Apr) The nature of hydrogen bonding in protic ionic liquids. Angew Chem Int Ed 52(17):4623–4627. John Wiley & Sons, Ltd. [Online]. Available: https://doi.org/10.1002/anie.201209273
152. Low K, Tan SYS, Izgorodina EI (2019) An ab initio study of the structure and energetics of hydrogen bonding in ionic liquids. Front Chem 7. [Online]. Available: https://www.frontiersin.org/articles/10.3389/fchem.2019.00208
153. Greaves TL, Drummond CJ (2008 Jan) Protic ionic liquids: properties and applications. Chem Rev 108(1):206–237. American Chemical Society. [Online]. Available: https://doi.org/10.1021/cr068040u
154. Allen MP, Tildesley DJ (2017) Computer simulation of liquids. Oxford University Press, New York, NY
155. Frenkel D, Smit B (2002) Frenkel D, Smit BBTUMSSE (eds) Understanding molecular simulation: from algorithms to applications. Academic Press. [Online]. Available: http://www.sciencedirect.com/science/article/pii/B9780122673511500031
156. Braun E, Gilmer J, Mayes HB, Mobley DL, Monroe JI, Prasad S, Zuckerman DM (2019) Best practices for foundations in molecular simulations [article v1.0]. Living J Comput Mol Sci 1(1):5957–5957. [Online]. Available:https://livecomsjournal.org/index.php/livecoms/article/view/v1i1e5957
157. Maginn EJ, Messerly RA, Carlson DJ, Roe DR, Elliot JR (2019) Best practices for computing transport properties 1. Self-diffusivity and viscosity from equilibrium molecular dynamics [article v1.0]. Living J Comput Mol Sci 1(1):6324–6324. [Online]. Available: https://livecomsjournal.org/index.php/livecoms/article/view/v1i1e6324
158. Chen S, Voth GA (2023 Feb) How does electronic polarizability or scaled-charge affect the interfacial properties of room temperature ionic liquids? The J Phys Chem B 127(5):1264–1275. American Chemical Society. [Online]. Available: https://doi.org/10.1021/acs.jpcb.2c07981
159. Dreher T, Lemarchand C, Soulard L, Bourasseau E, Malfreyt P, Pineau N (2018 Jan) Calculation of a solid/liquid surface tension: a methodological study. The J Chem Phys 148(3):034702. [Online]. Available: https://doi.org/10.1063/1.5008473
160. von Bülow S, Bullerjahn JT, Hummer G (2020 Jul) Systematic errors in diffusion coefficients from long-time molecular dynamics simulations at constant pressure. The J Chem Phys 153(2):021101. [Online]. Available: https://doi.org/10.1063/5.0008316
161. Basconi JE, Shirts MR (2013 Jul) Effects of temperature control algorithms on transport properties and kinetics in molecular dynamics simulations. J Chem Theory Computation 9(7):2887–2899. American Chemical Society. [Online]. Available: https://doi.org/10.1021/ct400109a
162. Zhang Y, Otani A, Maginn EJ (2015 Aug) Reliable viscosity calculation from equilibrium molecular dynamics simulations: a time decomposition method. J Chem Theory Computation 11(8):3537–3546. American Chemical Society. [Online]. Available: https://doi.org/10.1021/acs.jctc.5b00351
163. Ghorai PK, Matyushov DV (2020 May) Equilibrium solvation, electron-transfer reactions, and Stokes-shift dynamics in ionic liquids. The J Phys Chem B 124(18):3754–3769. American Chemical Society. [Online]. Available: https://doi.org/10.1021/acs.jpcb.0c01773
164. McDaniel JG, Verma A (2019 Jun) On the miscibility and immiscibility of ionic liquids and water. The J Phys Chem B 123(25):5343–5356. American Chemical Society. [Online]. Available: https://doi.org/10.1021/acs.jpcb.9b02187
165. Parmar SM, Depew DD, Wirz RE, Vaghjiani GL (2023 Oct) Structural properties of HEHN- and HAN-Based ionic liquid mixtures: a polarizable molecular dynamics study. The J Phys Chem B 127(40):8616–8633. American Chemical Society. [Online]. Available: https://doi.org/10.1021/acs.jpcb.3c02649
166. Sasse RA, Davies MA, Fifer RA, Decker MM, Kotlar AJ (1988 Dec) Density of HYDROXYLAMMONIUM nitrate solutions. Tech. Rep.," US Army Ballistic Research Laboratory
167. Klein N (1990 Aug) The molecular structure of the HAN -based liquid propellants. Tech. Rep.," US Army Ballistic Research Laboratory, Aberdeen Proving Ground
168. Freudenmann D, Ciezki HK (2019 Sep) ADN and HAN-Based monopropellants – a minireview on compatibility and Chemical stability in aqueous media. Propellants, Explos, Pyrotech 44(9):1084–1089. John Wiley & Sons, Ltd. [Online]. Available: https://doi.org/10.1002/prep.201900127
169. Lopes JNC, Esperança JMSS, Ferro AMD, Pereiro AB, Plechkova NV, Rebelo LPN, Seddon KR, Vázquez-Fernández I (2016 Mar) Protonic ammonium nitrate ionic liquids and their mixtures: insights into their thermophysical behavior. The J Phys Chem B 120(9):2397–2406. American Chemical Society. [Online]. Available: doi:https://doi.org/10.1021/acs.jpcb.5b11900
170. Castejón HJ, Lashock RJ (2012) Mixtures of ionic liquids with similar molar volumes form regular solutions and obey the cross-square rules for electrolyte mixtures. J Mol Liq 167:1–4. [Online]. Available: https://www.sciencedirect.com/science/article/pii/S0167732211003874
171. Gutowski KE, Gurkan B, Maginn EJ (2009 Oct) Force field for the atomistic simulation of the properties of hydrazine, organic hydrazine derivatives, and energetic hydrazinium ionic liquids. Pure And Appl Chem 81(10):1799–1828. [Online]. Available: https://doi.org/10.1351/PAC-CON-08-09-24
172. Roy D, Patel N, Conte S, Maroncelli M (2010 Jul) Dynamics in an idealized ionic liquid Model. The J Phys Chem B 114(25):8410–8424. American Chemical Society. [Online]. Available: https://doi.org/10.1021/jp1004709
173. Cardoso PF, Fernandez JSLC, Lepre LF, Ando RA, Gomes MFC, Siqueira LJA (2018 Apr) Molecular dynamics simulations of polyethers and a quaternary ammonium ionic liquid as CO2 absorbers. The J Chem Phys 148(13):134908. [Online]. Available: https://doi.org/10.1063/1.5019431
174. Weingärtner H (2008) Understanding ionic liquids at the molecular level: facts, problems, and controversies. Angew Chem Int Ed 47(4):654–670. eprint:https://onlinelibrary.wiley.com/doi/pdf/10.1002/anie.200604951. [Online]. Available
175. Schmidt EWEW (1984) Hydrazine and its derivatives : preparation, properties, applications. John Wiley & Sons, New York
176. Hunt PA, Ashworth CR, Matthews RP (2015) Hydrogen bonding in ionic liquids. Chem Soc Rev 44(5):1257–1288. The Royal Society of Chemistry. [Online]. Available: https://doi.org/10.1039/C4CS00278D
177. Jeffrey GA (1997) An introduction to hydrogen bonding. Oxford University Press
178. Lee H, Litzinger TA (2003) Chemical kinetic study of HAN decomposition. Combust And Flame 135(1):151–169. [Online]. Available: https://www.sciencedirect.com/science/article/pii/S0010218003001573
179. Ferguson RE, Esparza AA, Chambreau SD, Vaghjiani GL, Shafirovich E (2021 Aug) Studies on the combustion of HAN/Methanol/Water propellants and decomposition of HAN and HEHN. Int J Energetic Mater And Chem Propul 20(2):21–31. [Online]. Available: https://app.dimensions.ai/details/publication/pub.1135760923
180. Alavi S, Thompson DL (2003 Aug) Hydrogen bonding and proton transfer in small hydroxylammonium nitrate clusters: a theoretical study. The J Chem Phys 119(8):4274–4282. American Institute of Physics. [Online]. Available: https://doi.org/10.1063/1.1593011

181. Chambreau SD, Popolan-Vaida DM, Kostko O, Lee JK, Zhou Z, Brown TA, Jones P, Shao K, Zhang J, Vaghjiani GL, Zare RN, Leone SR (2022 Jan) Thermal and catalytic decomposition of 2-Hydroxyethylhydrazine and 2-hydroxyethylhydrazinium nitrate ionic liquid. The J Phys Chem A 126(3):373–394. American Chemical Society. [Online]. Available: https://doi.org/10.1021/acs.jpca.1c07408
182. Patrick AL, Vogelhuber KM, Prince BD, Annesley CJ (2018 Mar) Theoretical and experimental insights into the dissociation of 2-hydroxyethylhydrazinium nitrate clusters formed via electrospray. The J Phys Chem A 122(8):1960–1966. American Chemical Society. [Online]. Available: https://doi.org/10.1021/acs.jpca.7b12072
183. Zeng HJ, Khuu T, Chambreau SD, Boatz JA, Vaghjiani GL, Johnson MA (2020 Dec) Ionic liquid clusters generated from electrospray thrusters: cold ion spectroscopic signatures of size-dependent acid–Base interactions. The J Phys Chem A 124(50): 10507–10516. American Chemical Society. [Online]. Available: https://doi.org/10.1021/acs.jpca.0c07595
184. Zhou W, Liu J, Chambreau SD, Vaghjiani GL (2022) Structures, proton transfer and dissociation of hydroxylammonium nitrate (HAN) revealed by electrospray ionization tandem mass spectrometry and molecular dynamics simulations. Phys Chem Chem Phys 24(22):14033–14043. The Royal Society of Chemistry. [Online]. Available: http://dx.doi.org/10.1039/D2CP01571D

Publisher's Note